



# Mitochondria control store-operated $\text{Ca}^{2+}$ entry through $\text{Na}^+$ and redox signals

Tsipi Ben-Kasus Nissim<sup>1,‡</sup>, Xuexin Zhang<sup>2,‡</sup>, Assaf Elazar<sup>1</sup>, Soumitra Roy<sup>1</sup>, Judith A Stolwijk<sup>2</sup>, Yandong Zhou<sup>2</sup>, Rajender K Motiani<sup>2,†</sup>, Maxime Gueguinou<sup>2</sup>, Nadine Hempel<sup>3</sup>, Michal Hershinkel<sup>1</sup>, Donald L Gill<sup>2</sup>, Mohamed Trebak<sup>2,\*</sup>  & Israel Sekler<sup>1,\*\*</sup> 

## Abstract

Mitochondria exert important control over plasma membrane (PM) Orai1 channels mediating store-operated  $\text{Ca}^{2+}$  entry (SOCE). Although the sensing of endoplasmic reticulum (ER)  $\text{Ca}^{2+}$  stores by STIM proteins and coupling to Orai1 channels is well understood, how mitochondria communicate with Orai1 channels to regulate SOCE activation remains elusive. Here, we reveal that SOCE is accompanied by a rise in cytosolic  $\text{Na}^+$  that is critical in activating the mitochondrial  $\text{Na}^+/\text{Ca}^{2+}$  exchanger (NCLX) causing enhanced mitochondrial  $\text{Na}^+$  uptake and  $\text{Ca}^{2+}$  efflux. Omission of extracellular  $\text{Na}^+$  prevents the cytosolic  $\text{Na}^+$  rise, inhibits NCLX activity, and impairs SOCE and Orai1 channel current. We show further that SOCE activates a mitochondrial redox transient which is dependent on NCLX and is required for preventing Orai1 inactivation through oxidation of a critical cysteine (Cys195) in the third transmembrane helix of Orai1. We show that mitochondrial targeting of catalase is sufficient to rescue redox transients, SOCE, and Orai1 currents in NCLX-deficient cells. Our findings identify a hitherto unknown NCLX-mediated pathway that coordinates  $\text{Na}^+$  and  $\text{Ca}^{2+}$  signals to effect mitochondrial redox control over SOCE.

**Keywords** CRAC channel; mitochondrial redox; NCLX; SOCE; sodium signaling

**Subject Categories** Membrane & Intracellular Transport; Metabolism

**DOI** 10.15252/emboj.201592481 | Received 7 July 2015 | Revised 25 December

2016 | Accepted 5 January 2017 | Published online 20 February 2017

**The EMBO Journal (2017) 36: 797–815**

## Introduction

The store-operated  $\text{Ca}^{2+}$  entry (SOCE) pathway mediating the highly  $\text{Ca}^{2+}$  selective  $\text{Ca}^{2+}$  release-activated  $\text{Ca}^{2+}$  (CRAC) current is the major  $\text{Ca}^{2+}$  influx route in non-excitable cells (Putney, 1986; Potier & Trebak, 2008). The pathway is activated by interaction between the plasma membrane  $\text{Ca}^{2+}$  entry channel, Orai1 (Feske

*et al*, 2006; Vig *et al*, 2006; Zhang *et al*, 2006), and the endoplasmic reticulum (ER)  $\text{Ca}^{2+}$  sensor protein, STIM1 (Liou *et al*, 2005; Zhang *et al*, 2005). Numerous studies have revealed that mitochondria are also key regulators of SOCE activity (Hoth *et al*, 1997; Deak *et al*, 2014). However, the exact mechanisms by which mitochondria facilitate SOCE are poorly understood. With the steep mitochondrial membrane potential as its driving force,  $\text{Ca}^{2+}$  permeates into the mitochondrial matrix via the recently identified mitochondrial  $\text{Ca}^{2+}$  uniporter (MCU; Baughman *et al*, 2011; De Stefani *et al*, 2011; Patron *et al*, 2013).  $\text{Ca}^{2+}$  is extruded from the mitochondria by an electrogenic mitochondrial  $3\text{Na}^+/1\text{Ca}^{2+}$  exchanger (NCLX; Palty *et al*, 2010) which is powered by the same mitochondrial membrane potential. This constant cycling of  $\text{Ca}^{2+}$  in and out of mitochondria functions as a dynamic and important signaling link between cytosolic  $\text{Ca}^{2+}$  signals and metabolic activity maintained by the regulation of key Krebs cycle enzymes as well as the F1/F0-ATPase pump (Szabadkai & Duchon, 2008). The NCLX is a member of superfamily of  $\text{Na}^+/\text{Ca}^{2+}$  exchangers and shares with them the hallmark of  $\alpha 1/\alpha 2$  repeats that form the catalytic cation transport domain. It belongs to a distinct branch of this family termed CAX and is the single representative of this group in mammalian cells (Lytton, 2007; He & O'Halloran, 2014). It also has a unique selectivity to monovalent cations being capable of transporting either  $\text{Li}^+$  or  $\text{Na}^+$  in exchange for  $\text{Ca}^{2+}$ , while other members of the family are inert to  $\text{Li}^+$  (Palty *et al*, 2010). Because the mitochondrial  $\text{Ca}^{2+}$  efflux rate is 2–3 orders of magnitude slower than the rate of mitochondrial  $\text{Ca}^{2+}$  influx, the efflux represents a rate limiting step controlling the duration and magnitude of mitochondrial  $\text{Ca}^{2+}$  transients (Rudolf *et al*, 2004). In addition, by virtue of transporting at least 3  $\text{Na}^+$  per 1  $\text{Ca}^{2+}$ , NCLX is the major mitochondrial  $\text{Na}^+$  influx pathway (Baysal *et al*, 1994; Jung *et al*, 1995; Nita *et al*, 2014a). In fact, the affinity of the NCLX for  $\text{Na}^+$  is  $\sim 10$  mM and is therefore highly tuned to minor changes in cytosolic  $\text{Na}^+$  (Nita *et al*, 2014a).

Studies utilizing metabolic inhibitors and NCLX blockers suggest that mitochondria exert crucial regulation of CRAC channel

1 The Department of Physiology and Cell Biology, Faculty of Health Sciences, Ben-Gurion University of the Negev, Beer-Sheva, Israel

2 Department of Cellular and Molecular Physiology, The Pennsylvania State University College of Medicine, Hershey, PA, USA

3 Department of Pharmacology, The Pennsylvania State University College of Medicine, Hershey, PA, USA

\*Corresponding author. Tel: +1 717 531 8152; E-mail: mtrebak@psu.edu

\*\*Corresponding author. Tel: +972 8 6477328; E-mail: sekler@bgu.ac.il

‡These authors contributed equally to this work

†Present address: Systems Biology Group, CSIR-Institute of Genomics and Integrative Biology, New Delhi, India

activity (Malli *et al*, 2003; Ardon *et al*, 2009; Feldman *et al*, 2010). In immune cells, mitochondria are closely associated with the ER-PM junctions in which CRAC channels function (Hoth *et al*, 1997; Rizzuto *et al*, 1998, 2012; Alvarez *et al*, 1999; Berridge *et al*, 2003; Singaravelu *et al*, 2011). Because of their spatial proximity and  $\text{Ca}^{2+}$  shuttling capacity, it was proposed that mitochondria buffer  $\text{Ca}^{2+}$  at the vicinity of CRAC channels thus eliminating the well-established  $\text{Ca}^{2+}$ -dependent inactivation of the CRAC pathway (Parekh, 2008; Demaurex *et al*, 2009). However, in other cell types, for example, endothelial cells, mitochondria are more remotely located and are therefore less likely to directly buffer  $\text{Ca}^{2+}$  in the vicinity of CRAC channels (Demaurex *et al*, 2009; Giacomello *et al*, 2010; Naghdi *et al*, 2010; Nunes & Demaurex, 2014). Yet, remarkably, even in these cell types, the mitochondria can still impinge on CRAC activity through an as yet unidentified mechanism.

Interestingly, SOCE is also closely associated with the regulation of cytosolic  $\text{Na}^+$  and many studies have demonstrated that  $\text{Na}^+$  influx, mediated by non-selective transient receptor potential canonical (TRPC) channel members, occurs in response to receptor-mediated activation of CRAC channels (Lemos *et al*, 2007; Baryshnikov *et al*, 2009; Lee *et al*, 2010). Thus,  $\text{Na}^+$  signaling events are closely associated with SOCE and communication with mitochondria as recently reported (Reyes *et al*, 2013); however, the regulatory basis of this interaction remains poorly understood. SOCE is also strongly regulated by redox signals. These control several key steps including the interaction between STIM1 and Orai1 (Hawkins *et al*, 2010), and  $\text{Ca}^{2+}$  permeation by the Orai1 channel through modification of a redox-sensitive cysteine located on the Orai1 channel (Bogeski *et al*, 2010). Despite the fact that mitochondria are the major effectors of cellular redox, it is still not understood how mitochondrial redox impacts SOCE activity and mitochondrial  $\text{Ca}^{2+}$  signaling.

In the current study, we have sought to understand the cross talk between NCLX and SOCE. We reveal that expression of NCLX is required for SOCE and CRAC channel regulation through a mitochondrial proximity-independent pathway. We show that such regulation does not involve the elimination of  $\text{Ca}^{2+}$ -dependent inactivation of CRAC channels through mitochondrial buffering of  $\text{Ca}^{2+}$ . We found instead that integrated  $\text{Ca}^{2+}$  and  $\text{Na}^+$  signals act synergistically to promote mitochondrial  $\text{Ca}^{2+}$  shuttling that modulates mitochondrial redox status, thereby controlling SOCE activity.

## Results

### SOCE and CRAC currents are regulated by mitochondrial NCLX

To determine the role of the mitochondrial  $\text{Na}^+/\text{Ca}^{2+}$  exchanger, NCLX, we reduced its expression in HEK293T cells using previously characterized siNCLX (Palty *et al*, 2010). Consistent with previous results, HEK293T cells transfected with siNCLX displayed over twofold reduction in expression of NCLX protein compared to siControl cells with no significant change in the expression of STIM1 and Orai1 (Fig 1A). To determine the effect of NCLX knockdown on SOCE, we measured  $\text{Ca}^{2+}$  influx in Fura-2-loaded cells after depleting ER  $\text{Ca}^{2+}$  stores with  $\text{Ca}^{2+}$ -free Ringer containing ATP (100  $\mu\text{M}$ ) and thapsigargin (TG; 1  $\mu\text{M}$ ) followed by superfusion with

$\text{Ca}^{2+}$ -containing solutions (1.8 mM) while monitoring the rate of  $\text{Ca}^{2+}$  influx. Silencing of NCLX expression led to a 2.4-fold reduction in  $\text{Ca}^{2+}$  influx rate ( $*P < 0.05$ ) compared to cells transfected with siControl (1.2E-02 versus 5E-03; Fig 1B). As an additional strategy, we have employed the same experimental paradigm in cells expressing the plasma membrane-targeted  $\text{Ca}^{2+}$  probe, GCamp5 (Akerboom *et al*, 2012) to determine the localized change in  $\text{Ca}^{2+}$  concentration at the vicinity of the plasma membrane. This localized  $\text{Ca}^{2+}$  influx signal in siNCLX-transfected cells was also strongly (10-fold) reduced compared to  $\text{Ca}^{2+}$  signals observed in siControl-transfected cells (1.16E-03 versus 1.1E-04;  $*P < 0.05$ ; Fig 1C). However, NCLX knockdown had no effect on STIM1 and Orai1 protein expression determined by Western blotting (Fig 1A). To directly establish whether NCLX has a role in controlling SOCE thereby ruling out indirect effects of cellular  $\text{Ca}^{2+}$  pumping or changes in membrane potential, we measured store depletion-activated CRAC currents by whole-cell electrophysiological recordings (Fig 1D–F). CRAC currents were recorded in  $\text{Ca}^{2+}$ -containing bath solutions and further amplified by exchanging bath solutions with divalent-free (DVF). Such replacement immediately after break-in (first DVF exchange) led to the appearance of a relatively small linear  $\text{Na}^+$  current, reflecting cell membrane or seal leak due to the absence of divalent cations (Fig 1D). During subsequent DVF exchanges,  $\text{Ca}^{2+}$  store depletion had taken place and the DVF inward current increased steadily while the outward current remain unchanged. In such experiments, the leak subtracted store depletion-activated CRAC current recorded in DVF bath solution, displayed inward rectification typical of CRAC currents measured in  $\text{Ca}^{2+}$ -containing bath solutions. These CRAC  $\text{Na}^+$  currents also showed the typical rapid depotentiation in DVF bath solutions (Fig 1D). The current–voltage (I–V) relationships revealed inward rectification with a highly positive reversal potential and complete block by low concentrations of lanthanides (5  $\mu\text{M}$   $\text{Gd}^{3+}$ ; Fig 1D), consistent with the properties of CRAC currents recorded in many other cells. Just as NCLX knockdown reduced the store-operated  $\text{Ca}^{2+}$  entry response, it also led to a twofold–threefold inhibition of both CRAC-mediated  $\text{Ca}^{2+}$  and  $\text{Na}^+$  currents (Fig 1E and F). To determine whether the NCLX-dependent changes in SOCE and CRAC are mediated by a change in STIM1–Orai1 interactions, we monitored co-localization of STIM1–YFP and Orai1–CFP. We determined that puncta formation after store depletion (Fig 2A and B) as well as enhanced STIM1–Orai1 FRET (Fig 2C) was not affected by NCLX knockdown. Importantly, the time course of STIM1/Orai1 FRET interaction upon store depletion is indistinguishable between siControl and siNCLX cells (Fig EV1 and Movies EV1 and EV2). In contrast to the inhibitory effects that NCLX knockdown had on  $\text{Ca}^{2+}$  signals and CRAC current, the knockdown of MCU did not inhibit SOCE and CRAC currents in HEK293T cells (Appendix Fig S1).

Cultured primary aortic vascular smooth muscle cells (VSMCs) display robust SOCE as previously characterized in detail (Potier *et al*, 2009). We sought to determine whether similar cross talk between SOCE and mitochondrial NCLX exists in these cells. Silencing of NCLX expression led to a fourfold reduction in store-operated  $\text{Ca}^{2+}$  influx rate measured with Fura-2 ( $*P < 0.05$ ) compared to cells transfected with siControl (2.1E-03 versus 5.2E-04; Fig 3A). The electrophysiological recordings of CRAC currents in VSMCs also showed twofold–threefold reduction in CRAC current density upon

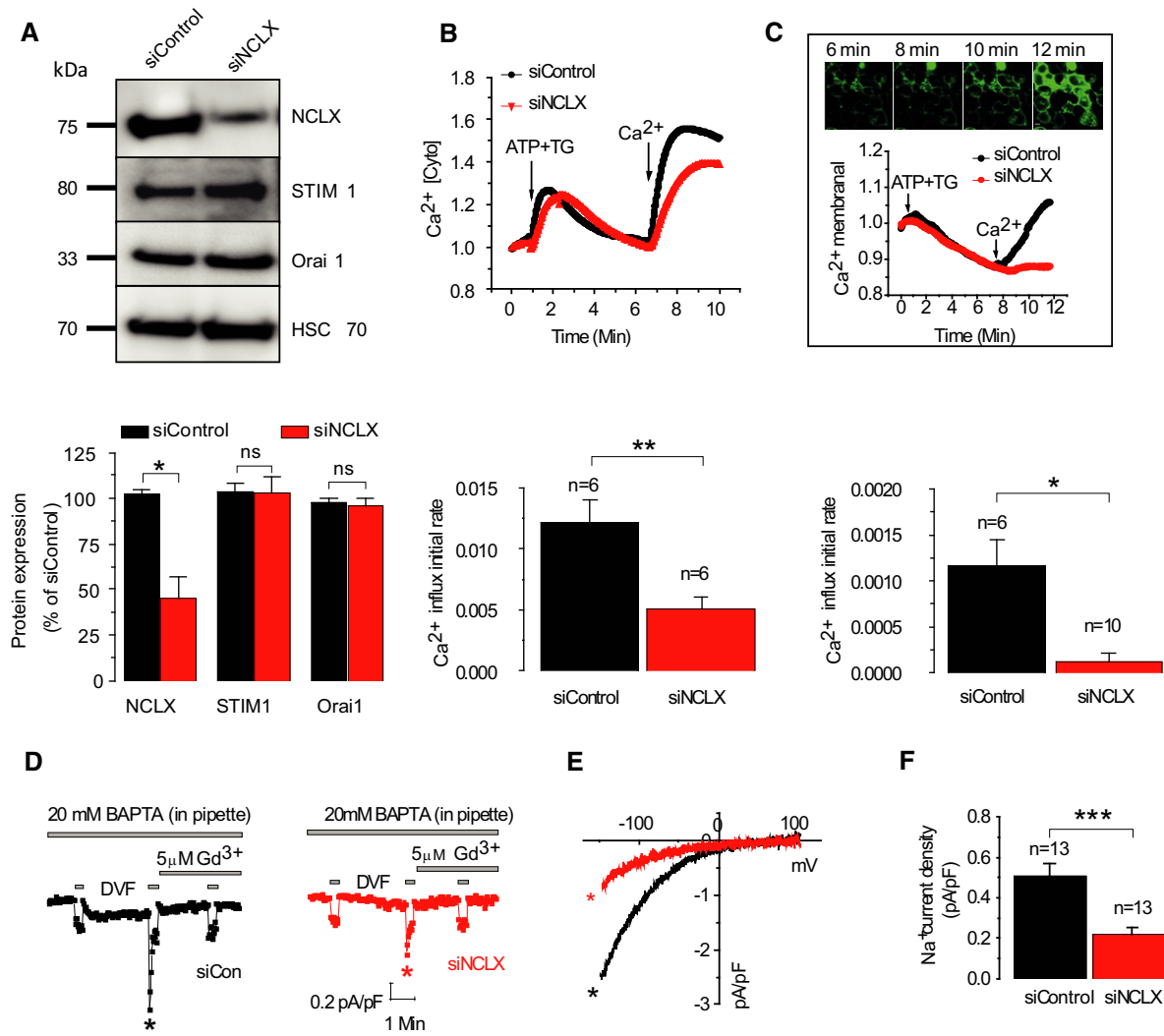


**Figure 1. NCLX controls SOCE activity.**

- A Upper panel: Western blot was performed with 100 μg of protein samples obtained from HEK293T cells transfected with either siControl or siNCLX. Lower panel: Densitometry analysis of immunoblots of siControl-transfected cells ( $n = 3$ ) versus siNCLX-transfected cells ( $n = 3$ ) representing normalized expression levels (% of control) of NCLX, STIM1 and Orai1.
- B Upper panel: HEK293T cells were transfected with either scrambled siRNA construct (siControl, black) or siNCLX (red) and loaded with Fura-2. SOCE was triggered by ATP (100 μM) and thapsigargin (TG, 1 μM), and Fura-2 fluorescence was monitored as described in Materials and Methods. Lower panel: Averaged rates of Ca<sup>2+</sup> rise in siNCLX-silenced cells from several independent recordings ( $n = 6$ ) versus siControl-transfected cells ( $n = 6$ ).
- C Upper panel: Fluorescence of the membrane calcium sensor, GCaMP5, targeted to the plasma membrane following treatment as described above using confocal microscopy. The scale bar represents 10 μm. Middle panel: Traces of membrane-localized Ca<sup>2+</sup> responses were measured in HEK293T cells co-transfected with either the siNCLX (red) or siControl (black) and GCaMP5-expressing plasmid. The lower panel shows the averaged rates of membrane-localized Ca<sup>2+</sup> rise either in siControl cells ( $n = 6$ ) or siNCLX cells ( $n = 10$ ).
- D Electrophysiological recordings were performed on the same batch of transfected cells used for Western blot and shown in panel (A). Representative time courses of whole-cell CRAC currents activated by dialysis of 20 mM BAPTA through the patch pipette and taken at -100 mV from cells transfected either with siControl (black trace) or siNCLX (red trace).
- E Representative I-V relationships are taken from traces in (D) where indicated by color-coded asterisks.
- F Statistical analysis on Na<sup>+</sup> CRAC currents measured at -100 mV is shown.

Data information: The results are presented as the means ± SEM. \* $P < 0.05$ ; \*\* $P < 0.01$ ; \*\*\* $P < 1E-03$ .  $P$ -values indicate the results of an unpaired Student's  $t$ -test. Source data are available online for this figure.

NCLX knockdown (Fig 3B and C). Together, these results indicate that mitochondrial NCLX is required for optimal activation of SOCE and CRAC currents.

Mitochondrial control of store-operated Ca<sup>2+</sup> signaling is known to occur as a result of buffering the Ca<sup>2+</sup> entering through CRAC channels by virtue of the close proximity of mitochondria to

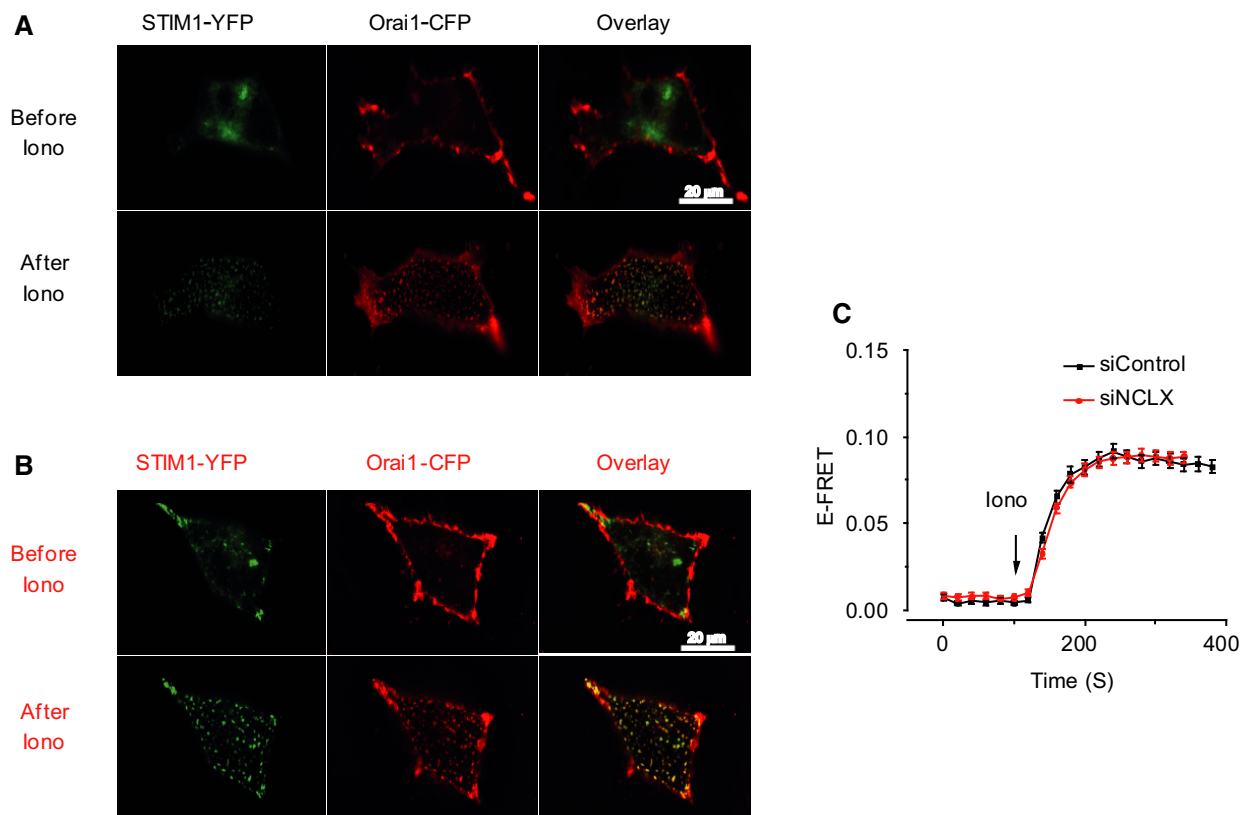


**Figure 2. NCLX knockdown has no effect on Orai1 and STIM1 interaction following store depletion.**

A, B HEK293T cells stably expressing Orai1-CFP and STIM1-YFP were transfected with either control siRNA (A) or NCLX siRNA (B) and incubated for 72 h. E-FRET experiments were then performed. The scale bar represents 20  $\mu\text{m}$ .

C Silencing of NCLX by siNCLX (red) has no effect on Orai1 and STIM1 colocalization after store depletion induced by applying 2.5  $\mu\text{M}$  ionomycin to the bath solution, compared to siControl (black; means  $\pm$  SEM).

the channels (Glitsch *et al*, 2002). This mode of regulation is revealed when CRAC channel activation is measured in the presence of low  $\text{Ca}^{2+}$  buffer in the patch pipette (e.g. 0.1 mM EGTA). In contrast, other studies suggested that an elusive proximity-independent mechanism is mediating mitochondrial regulation of CRAC channels (Giacomello *et al*, 2010; Pizzo *et al*, 2012). To address this, we determined whether NCLX regulation of CRAC current is dependent on  $\text{Ca}^{2+}$  buffering by analyzing CRAC current under varying cytosolic  $\text{Ca}^{2+}$  buffering conditions. Although the inhibitory effect of NCLX knockdown on CRAC channels persisted when CRAC channels were activated by a high concentration of a fast  $\text{Ca}^{2+}$  buffer (20 mM BAPTA; Figs 1 and 3), we considered that NCLX might be more intimately coupled to CRAC channels and therefore higher buffering capacity would be needed to recapitulate this close interaction. As shown in Fig 4A and B, the inhibitory effect of NCLX knockdown was essentially maintained whether 20 mM or 50 mM BAPTA was used indicating that NCLX is unlikely to be acting only through buffering cytosolic  $\text{Ca}^{2+}$  to relieve the  $\text{Ca}^{2+}$ -mediated negative feedback on CRAC channels. Thus, our results indicate that the regulation of SOCE by mitochondrial NCLX is at least partially mediated by a mechanism distinct from  $\text{Ca}^{2+}$  buffering in the vicinity of the mouth of CRAC channels.

A similar inhibitory effect of NCLX knockdown was observed in cells dialyzed with a mitochondrial-energizing solution (see Materials and Methods). Thus, when the mitochondrial-energizing cocktail was used, CRAC currents were 2.8-fold bigger than those recorded with conventional pipette solution (Fig EV2). Importantly, and consistently with the results described in Fig 4A and B, we found that even under conditions of energized mitochondria (and hence enhanced mitochondrial  $\text{Ca}^{2+}$  buffering), NCLX knockdown still inhibits CRAC current (Fig 4C–E), further supporting our conclusion that NCLX acts through a pathway independent of mitochondrial  $\text{Ca}^{2+}$  buffering.

#### Sodium transport by NCLX controls $\text{Ca}^{2+}$ influx via SOCE

One important distinction between NCLX and MCU is that the latter is solely a  $\text{Ca}^{2+}$  transporter while the former mediates exchange of three  $\text{Na}^+$  per  $\text{Ca}^{2+}$  ion and therefore exerts dual control of  $\text{Ca}^{2+}$  and  $\text{Na}^+$  transport (Pitts, 1979; Reeves & Hale, 1984). We asked whether  $\text{Na}^+$  plays a role in regulating SOCE by comparing the SOCE responses in cells superfused with bath solutions containing either physiological concentrations of  $\text{Na}^+$  (140 mM) or an equal concentration of NMDG<sup>+</sup>, a large monovalent cation that is not transported. Notably, replacing extracellular  $\text{Na}^+$  with NMDG<sup>+</sup> led

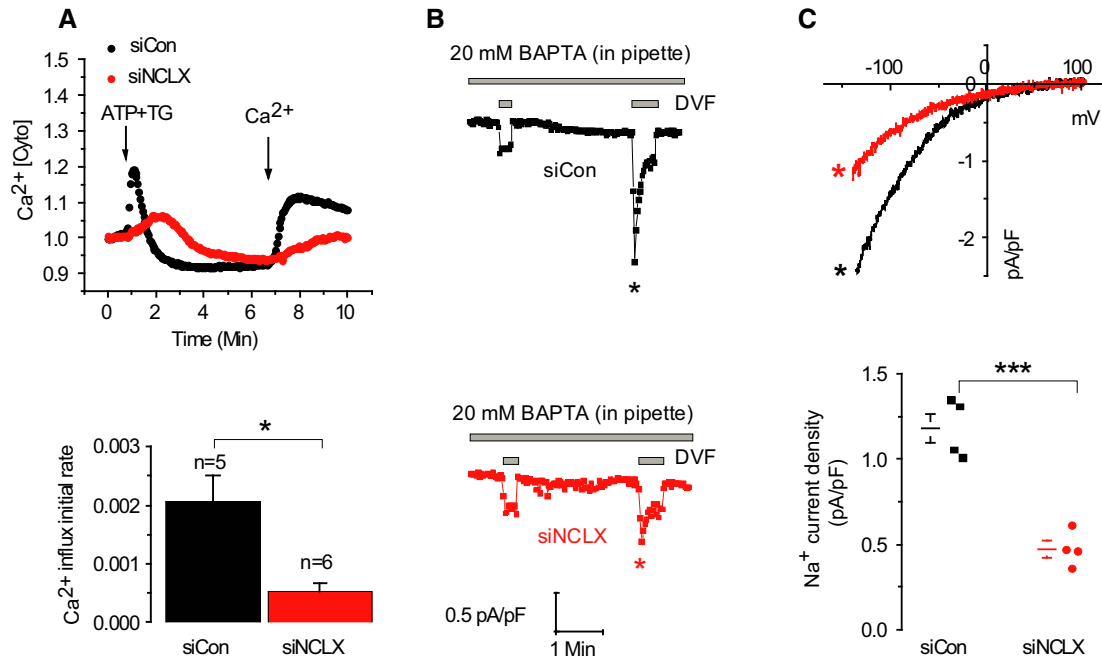


**Figure 3. Effect of NCLX knockdown on SOCE in primary vascular smooth muscle cells (VSMCs).**

A Upper panel: Fluorescence traces of cytosolic  $\text{Ca}^{2+}$  responses in VSMC cells. Lower panel: Averaged rates of cytosolic  $\text{Ca}^{2+}$  influx in siControl cells ( $n = 5$ ) and siNCLX cells ( $n = 6$ ).  
 B, C Electrophysiological CRAC recordings in cells as in (A) using the same protocol used in Fig 2. Statistical analysis on  $\text{Na}^+$  CRAC currents measured at  $-100$  mV is shown in (C).

Data information: The results are presented as the means  $\pm$  SEM. \* $P < 0.05$ ; \*\*\* $P < 1\text{E-}03$ .  $P$ -values indicate the results of an unpaired Student's  $t$ -test.

to a threefold decrease in store-operated  $\text{Ca}^{2+}$  influx rate (Fig 5A) [ $5\text{E-}03$  versus  $1.53\text{E-}02$ ; \*\*\* $P < 1\text{E-}03$ ]. However, when  $\text{Na}^+$  ions were replaced with  $\text{Li}^+$ , a substrate ion for NCLX but not of plasma membrane  $\text{Na}^+/\text{Ca}^{2+}$  exchanger (NCX; Palty *et al*, 2004), the store-dependent  $\text{Ca}^{2+}$  influx was rescued and was similar to that of the  $\text{Na}^+$ -containing Ringer solution ( $1.13\text{E-}02$  versus  $1.49\text{E-}02$ , respectively; Fig 5B, lower panel). Furthermore, silencing of NCLX expression combined with replacing  $\text{Na}^+$  ions in the Ringer's solutions with  $\text{NMDG}^+$  led to eightfold reduction in  $\text{Ca}^{2+}$  influx [ $1.49\text{E-}02$  and  $1.8\text{E-}03$ , respectively; \*\*\* $P < 1\text{E-}03$  (Fig 5B)]. To determine whether intracellular  $\text{Na}^+$  rise is required for SOCE activation, cytosolic  $\text{Na}^+$  rise was triggered by blocking the  $\text{Na}^+/\text{K}^+$  ATPase by preincubation with ouabain ( $100 \mu\text{M}$ ; Fig 5C) in the presence of  $\text{Na}^+$  to load the cytosol with  $\text{Na}^+$ . As expected, application of ouabain in the presence of extracellular  $\text{Na}^+$  led to an increase in cytosolic  $\text{Na}^+$  concentrations (Appendix Fig S2). We then compared the rates of store-dependent  $\text{Ca}^{2+}$  influx in cells initially pretreated with ouabain in the presence of  $\text{Na}^+$  and then superfused with  $\text{NMDG}^+$  (without  $\text{Na}^+$ ) versus untreated cells superfused with either  $\text{NMDG}^+$  or  $\text{Na}^+$ . Ouabain pretreatment in cells subsequently superfused with  $\text{NMDG}^+$ -containing bath solution had a similar effect of supporting SOCE to that of extracellular  $\text{Na}^+$  (Fig 5C, upper panel). Thus, preloading the cytosol with  $\text{Na}^+$  is sufficient for restoring store-dependent  $\text{Ca}^{2+}$  influx rate in  $\text{NMDG}^+$ -containing bath solutions to similar values as in  $\text{Na}^+$ -containing bath solutions ( $1.78\text{E-}02$  and  $1.41\text{E-}02$ , respectively; Fig 5C, lower panel), but not

in cells superfused with  $\text{NMDG}^+$  without preincubation with ouabain ( $8.5\text{E-}03$ , \*\* $P < 0.01$ ). This set of experiments indicates that the cytosolic rise in  $\text{Na}^+$  is required for full activation of SOCE.

We then asked whether a rise in cytosolic monovalent cations will have a similar effect on CRAC currents in HEK293T cells. Both solutions containing  $\text{Ca}^{2+}$  ( $20 \text{ mM}$ ) in the presence of the indicated cations ( $\text{Na}^+$ ,  $\text{NMDG}^+$  or  $\text{Li}^+$ ) were used to measure  $\text{Ca}^{2+}$  CRAC currents. The pipette solution contained  $0.1 \text{ mM}$  EGTA,  $\text{IP}_3$  to deplete stores, together with the mitochondrial-energizing cocktail described above. As shown in Fig 5D–G, the presence of either  $\text{Na}^+$  or the NCLX substrate  $\text{Li}^+$  in the bath solution led to development of inwardly rectifying  $\text{Ca}^{2+}$  CRAC currents that were blocked by  $5 \mu\text{M}$   $\text{Gd}^{3+}$ . However, replacing  $\text{Na}^+$  in the bath solution with  $\text{NMDG}^+$  inhibited  $\text{Ca}^{2+}$  CRAC current activation in response to store depletion by  $\text{IP}_3$ . A scatter blot representation of these data showing individual recordings with mean  $\pm$  SE is shown in Fig EV3.

We obtained similar results when CRAC currents were activated in either HEK293T cells (Fig EV3A and B) or rat basophilic leukemia cells (RBL; Fig EV3C). Recordings in HEK293T cells were performed under two conditions: either with store depletion achieved by inclusion of  $\text{IP}_3$  and mitochondrial-energizing cocktail together with  $0.1 \text{ mM}$  EGTA in the patch pipette (Fig EV3A) or with  $20 \text{ mM}$  BAPTA in the patch pipette (Fig EV3B) in the presence of either extracellular  $\text{Na}^+$  or  $\text{NMDG}^+$ . Although CRAC current was consistently inhibited by extracellular  $\text{NMDG}^+$  under all conditions,



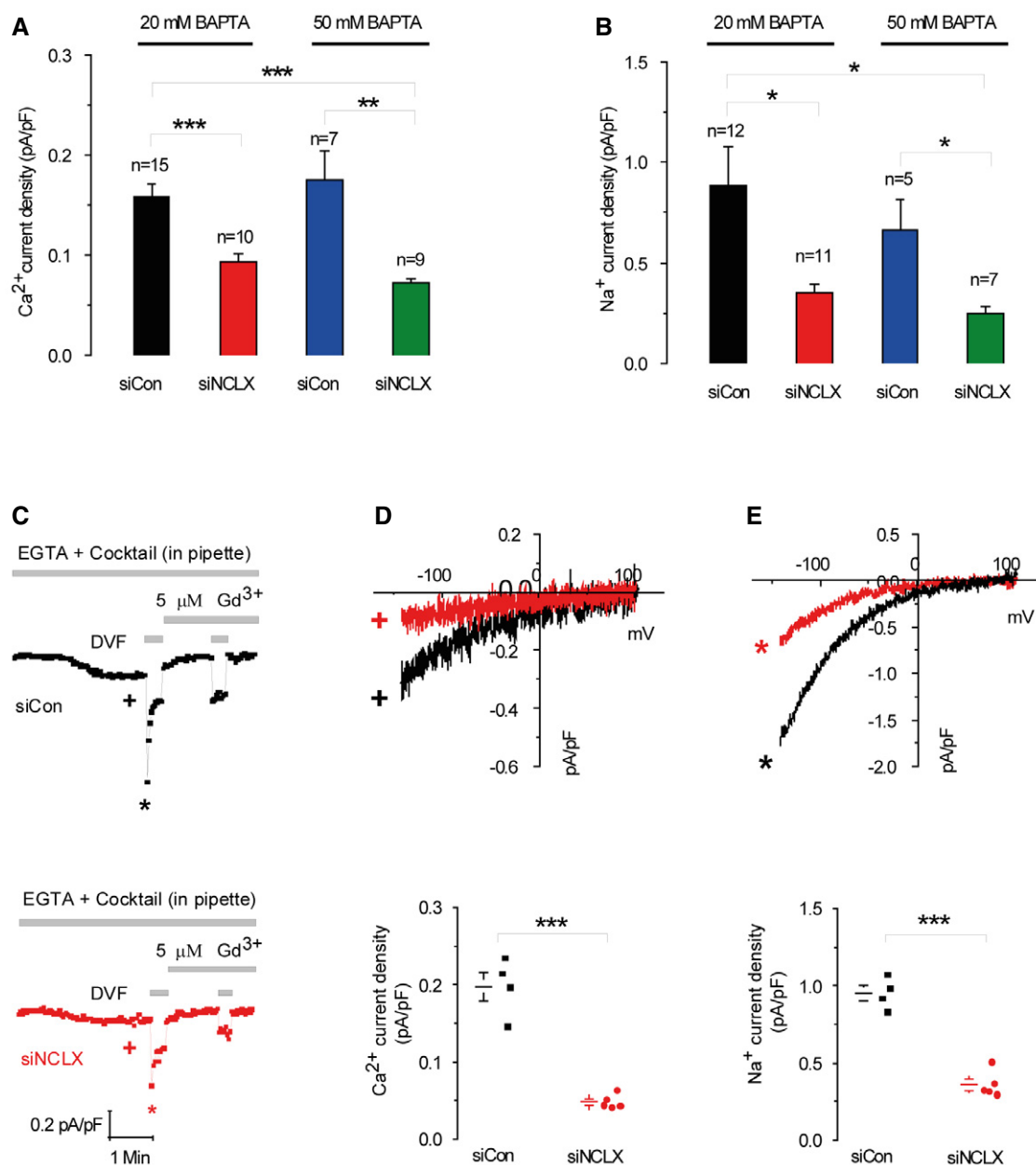


**Figure 4. NCLX does not control CRAC channels through buffering of cytosolic Ca<sup>2+</sup> or mitochondrial energization.**

A, B Analysis of Ca<sup>2+</sup> (A) and Na<sup>+</sup> (B) CRAC currents measured at  $-100$  mV in HEK293T cells transfected with either siControl or siNCLX using the indicated concentrations of BAPTA (20 mM versus 50 mM) in the pipette solution to activate CRAC and buffer cytosolic Ca<sup>2+</sup>.

C–E Electrophysiological CRAC recordings were performed on cells where store depletion was induced by the use of a pipette solution containing low buffering capacity (0.1 mM EGTA) with IP<sub>3</sub> (30  $\mu$ M) and a cocktail to energize the mitochondria whose composition is listed in the Results section. Representative time courses of whole-cell current development at  $-100$  mV (D, E) and measured in Ca<sup>2+</sup>-containing and DVF solutions, respectively, by comparison with siControl. At the end of recordings, 5  $\mu$ M Gd<sup>3+</sup> was used to inhibit CRAC currents. Representative I–V relationships of Ca<sup>2+</sup> (D) and Na<sup>+</sup> (E) CRAC in cells transfected with siControl or siNCLX are taken from traces in (C) where indicated by color-coded asterisks. Statistical analysis on Ca<sup>2+</sup> and Na<sup>+</sup> CRAC currents measured at  $-100$  mV (D, E).

Data information: The results are presented as the means  $\pm$  SEM. \* $P < 0.05$ ; \*\* $P < 0.01$ ; \*\*\* $P < 1E-03$ .  $P$ -values indicate the results of a one-way ANOVA test followed by Tukey *post hoc* analysis (A, B) or unpaired Student's *t*-test (C–E).

extracellular NMDG<sup>+</sup>-mediated inhibition of CRAC current was more pronounced when CRAC currents were activated by 0.1 mM EGTA together with 30  $\mu$ M IP<sub>3</sub> (Fig EV3A and B). Note that the slightly smaller potency of Li<sup>+</sup> versus Na<sup>+</sup> in stimulating CRAC and

SOCE is consistent with the lower exchange rate of Li<sup>+</sup> versus Na<sup>+</sup> mediated by NCLX (Carafoli *et al*, 1974). This corresponds to the functional fingerprint of NCLX and reveals that NCLX is the integrating component between Na<sup>+</sup> signaling and SOCE (Palty *et al*, 2004).

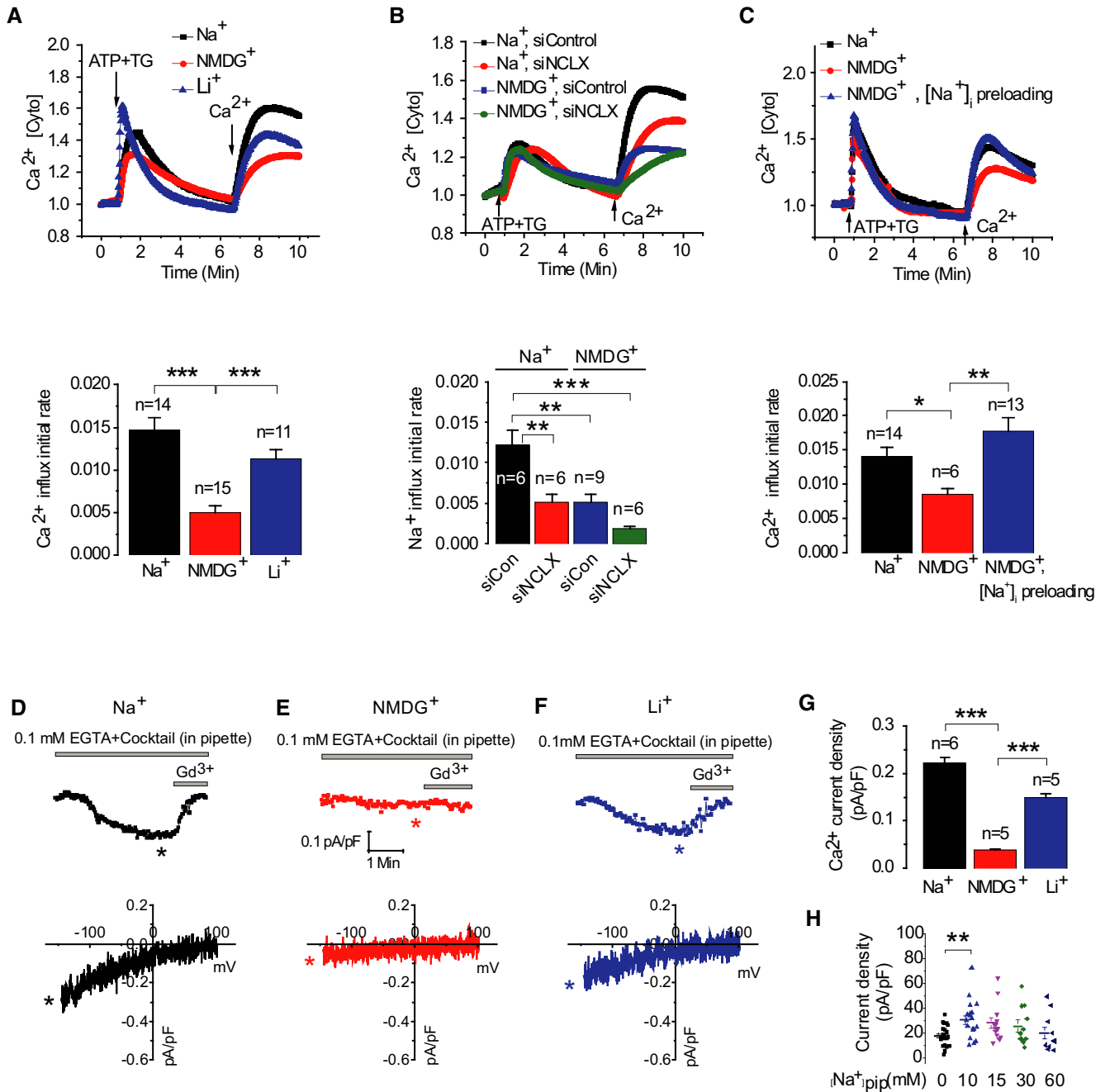


**Figure 5. Extracellular Na<sup>+</sup> signaling controls Ca<sup>2+</sup> influx through SOCE and CRAC channels.**

A, B Upper panel: Cytosolic Ca<sup>2+</sup>, Ca<sup>2+</sup> [Cyto], responses monitored in HEK293T cells after store depletion by ATP and TG as in Fig 1B and upon extracellular Na<sup>+</sup> ions replacement by either NMDG<sup>+</sup> or Li<sup>+</sup> ions. Lower panel: Averaged rates of cytosolic Ca<sup>2+</sup> influx. The combined effects of NMDG<sup>+</sup> together with silencing of NCLX on cytosolic Ca<sup>2+</sup> influxes via SOCE are presented in (B).

C Upper panel: After being loaded with Fura-2, intracellular Na<sup>+</sup>, [Na<sup>+</sup>]<sub>i</sub>, was preloaded by preincubation for 20 min with ouabain (100 μM) in the presence of Na<sup>+</sup>, following loading of intracellular Na<sup>+</sup> SOCE protocol was applied as in Fig 1 using NMDG<sup>+</sup>-containing Ringer. Lower panel: Averaged Ca<sup>2+</sup> influx rates in NMDG<sup>+</sup> [Na<sup>+</sup>]<sub>i</sub> preloaded cells (n = 6), Na<sup>+</sup> control cells (n = 14), and cells perfused with NMDG<sup>+</sup> alone (n = 13).

D–H Representative Ca<sup>2+</sup> CRAC current recordings and corresponding color-matched I–V relationships measured in HEK293T cells with different monovalent cation-based bath solution is shown in (D) for Na<sup>+</sup>, in (E) for NMDG<sup>+</sup>, and in (F) for Li<sup>+</sup>; 20 mM Ca<sup>2+</sup> was included in all bath solutions. Statistical analysis on Ca<sup>2+</sup> CRAC currents measured at –100 mV in all three conditions is shown in (G). The effects of cytosolic Na<sup>+</sup> concentration on Ca<sup>2+</sup> CRAC currents. (H) The whole-cell patch clamp recordings were performed in HEK293T cells transiently expressing eYFP-STIM1 and CFP-Orai1. Scatter plots represent Ca<sup>2+</sup> CRAC currents activated by dialysis through the patch pipette of a solution containing 20 mM BAPTA and the different concentration of Na<sup>+</sup>. Currents were measured at –100 mV and shown as current density pA/pF.

Data information: The results are presented as the means ± SEM. \*P < 0.05; \*\*P < 0.01 \*\*\*P < 1E-03. P-values indicate the results of a one-way ANOVA test followed by Tukey *post hoc* analysis.

To determine the role of intracellular  $\text{Na}^+$  in mediating the action of CRAC current, we performed another set of experiments in which HEK293T cells were co-transfected with STIM1 and Orai1 to generate large CRAC currents. Using these cells, whole-cell patch clamp recordings were performed after store depletion induced by dialysis with 20 mM BAPTA through the patch pipette together with bath solution containing 135 mM  $\text{Na}^+$  and 20 mM  $\text{Ca}^{2+}$  in the presence of varying concentrations of  $\text{Na}^+$  in the patch pipette (Fig 5H). HEK293T cells co-expressing STIM1 and Orai1 exhibited enhanced CRAC currents when the pipette solution contained 10 mM or higher  $\text{Na}^+$  concentrations (Fig 5H), providing additional support for the role of  $\text{Na}^+$  in optimal CRAC current activation.

Additional support for the cross talk between  $\text{Na}^+$  and  $\text{Ca}^{2+}$  ions on CRAC channel function was derived from direct monitoring of  $\text{Na}^+$  influx, applying the SOCE protocol to cells loaded with the fluorescent  $\text{Na}^+$  dye Asanta Natrium (Fig 6A and B). Depletion of  $\text{Ca}^{2+}$  stores triggered a 4.5-fold rise in  $\text{Na}^+$  influx rate compared to control cells with intact  $\text{Ca}^{2+}$  stores [ $2.60\text{E-}04$  and  $5.87\text{E-}05$ , respectively,  $**P < 0.01$ ] (Fig 6A, lower panel). This finding is consistent with previous studies documenting store-dependent  $\text{Na}^+$  influx (Poburko *et al*, 2009).  $\text{Na}^+$  influx was observed only in the presence of extracellular  $\text{Na}^+$  indicating that it reflects  $\text{Na}^+$  permeation into cells and not release from putative intracellular  $\text{Na}^+$  stores (Fig 6B, upper panel) [ $2\text{E-}04$  versus  $-3\text{E-}05$ ,  $**P < 0.01$ ] (Fig 6B, lower panel). We further asked whether the cytosolic  $\text{Na}^+$  rise is propagating into the mitochondria by monitoring changes in mitochondrial  $\text{Na}^+$  in cells preloaded with the mitochondrial  $\text{Na}^+$  reporter, CoroNa red (Jayaraman *et al*, 2001a,b). As shown in Fig 6C, SOCE activation was linked to a strong mitochondrial  $\text{Na}^+$  influx, consistent with the major role of NCLX in mediating mitochondrial  $\text{Na}^+$  uptake (Palty *et al*, 2010; Nita *et al*, 2014a). Mitochondrial  $\text{Na}^+$  uptake was however reduced in cells superfused with NMDG<sup>+</sup> Ringer compared to cells superfused with  $\text{Na}^+$ -containing Ringer, ( $2.3\text{E-}04$  and  $5\text{E-}04$ , respectively,  $*P < 0.05$ ; Fig 6C), indicating that mitochondrial  $\text{Na}^+$  influx is preceded by  $\text{Na}^+$  influx into the cell across the plasma membrane. Previous studies demonstrated that NCLX is tuned to sense small changes in cytosolic  $\text{Na}^+$  and is therefore strongly activated by a rise in cytosolic  $\text{Na}^+$  triggered, for example, by voltage gated  $\text{Na}^+$  channels in pancreatic  $\beta$  cells (Nita *et al*, 2014a). We therefore asked whether  $\text{Na}^+$  influx is activating SOCE by triggering activation of NCLX. We monitored mitochondrial  $\text{Ca}^{2+}$  extrusion via the mitochondrial NCLX (Palty *et al*, 2010) by performing the SOCE protocol as described in Fig 1 while monitoring mitochondrial  $\text{Ca}^{2+}$  in the absence or presence of extracellular  $\text{Na}^+$ . The presence of  $\text{Na}^+$  ions in the Ringer solution strongly accelerated mitochondrial  $\text{Ca}^{2+}$  efflux (Fig 6D, upper panel). In contrast, mitochondrial  $\text{Ca}^{2+}$  efflux rate was reduced by 2.5-fold in the presence of NMDG<sup>+</sup> compared to cells that were superfused with  $\text{Na}^+$ -containing Ringer ( $2.26\text{E-}04$  and  $5.7\text{E-}04$ , respectively,  $**P < 0.01$ , Fig 6D, lower panel).

Thus far, we determined that the mitochondrial  $\text{Ca}^{2+}$  efflux triggered by robust store depletion using ATP+TG is  $\text{Na}^+$  dependent. Next, we sought to determine whether this is also the case when SOCE is activated using more physiological means (i.e. with purinergic ATP stimulation alone; Fig 6E, upper panel). As expected, absence of  $\text{Na}^+$  led to twofold lower ATP-activated mitochondrial  $\text{Ca}^{2+}$  efflux than the control (with  $\text{Na}^+$ ;  $1.13\text{E-}04$  and  $5.13\text{E-}05$ , respectively,  $**P < 0.01$ , Fig 6E, lower panel) and the combination

of using NMDG<sup>+</sup> Ringer together with silencing NCLX resulted in the lowest  $\text{Ca}^{2+}$  efflux rate ( $-1.02\text{E-}06$ ). Silencing of NCLX alone shows 3.6-fold decrease in the  $\text{Ca}^{2+}$  efflux rate versus control ( $7.85\text{E-}04$  and  $2.18\text{E-}04$ , respectively; Fig EV4). As shown in Fig 6F, mitochondrial  $\text{Ca}^{2+}$  efflux following mitochondrial  $\text{Ca}^{2+}$  entry is strictly dependent on the presence of  $\text{Na}^+$ , consistent with our previous studies (Nita *et al*, 2014a).  $\text{Na}^+$  dose dependence analysis of mitochondrial  $\text{Ca}^{2+}$  efflux revealed an apparent  $K_m$  of 9.7 mM in HEK293T cells (Fig 6F), in agreement with values previously reported for cardiac myocytes (Cai *et al*, 2016) and consistent with  $\text{Na}^+$  physiological concentrations, which are typically within 4–16 mM range (Bers *et al*, 2003). Altogether our results indicate that  $\text{Ca}^{2+}$  influx through the SOCE pathway requires a cytosolic  $\text{Na}^+$  rise to propagate within mitochondria through the exchange activity of NCLX which activates mitochondrial  $\text{Ca}^{2+}$  efflux. The results further suggest that this  $\text{Na}^+$  is required for activating mitochondrial  $\text{Ca}^{2+}$  shuttling by NCLX hence ensuring optimal activation of SOCE and CRAC currents.

### SOCE and CRAC current are regulated by mitochondrial redox

Mitochondrial redox state is elicited by mitochondrial  $\text{Ca}^{2+}$  transients and in turn regulates SOCE. We reasoned that the NCLX knockdown effect on SOCE is mediated by mitochondrial redox (De Marchi *et al*, 2014). To determine whether NCLX knockdown affects mitochondrial redox state, we applied the SOCE protocol as described in Fig 1 in cells expressing the redox sensor roGFP1 targeted to the mitochondrial matrix. Store depletion by ATP and thapsigargin (TG) in the absence of external  $\text{Ca}^{2+}$  followed by addition of  $\text{Ca}^{2+}$  to the bath solution, triggered transient changes in the mitochondrial redox state, temporarily reducing mitochondrial free oxygen radical levels in the mitochondrial matrix (Fig 7A). In contrast, knockdown of NCLX expression was followed by a twofold inhibition of this redox change (Fig 7A). Consistent with the role of NCLX in controlling the mitochondrial redox state, the knockdown of NCLX was followed by a fivefold lower NADH/NAD<sup>+</sup> ratio, monitored by intrinsic fluorescence ( $2.4\text{E-}04$  and  $1.2\text{E-}03$ , respectively,  $*P < 0.05$ ; Fig 7B, lower panel). These results indicate that the redox transients maintained by NCLX limit free radical bursts and thereby prevent oxidant-mediated inhibition of SOCE/CRAC.

Hence, the SOCE/CRAC activity suppressed by NCLX knockdown could be rescued by mitochondrial targeted expression of an  $\text{H}_2\text{O}_2$ -metabolizing enzyme, mitochondrial catalase (m-catalase). We determined whether m-catalase can restore the mitochondrial redox response in NCLX-silenced cells. Note that the m-catalase expression fully rescued the SOCE-dependent increase in reduced state of the mitochondrial matrix (Fig 7C). We then compared SOCE rate in siControl versus siNCLX cells with or without m-catalase expression. Remarkably, overexpression of m-catalase in NCLX knockdown cells was sufficient to recover SOCE activity and  $\text{Ca}^{2+}$  influx rate (Fig 7D). Further support for the link between  $\text{Na}^+$  and NCLX in controlling SOCE by redox is demonstrated by our finding that expression of m-catalase rescued SOCE even in the absence of extracellular  $\text{Na}^+$  (Fig EV5).

We then asked whether the rescue of the mitochondrial redox transient by m-catalase could restore CRAC currents suppressed by knockdown of NCLX expression. Consistent with the above SOCE results (Fig 7C and D), we observed that knockdown of NCLX



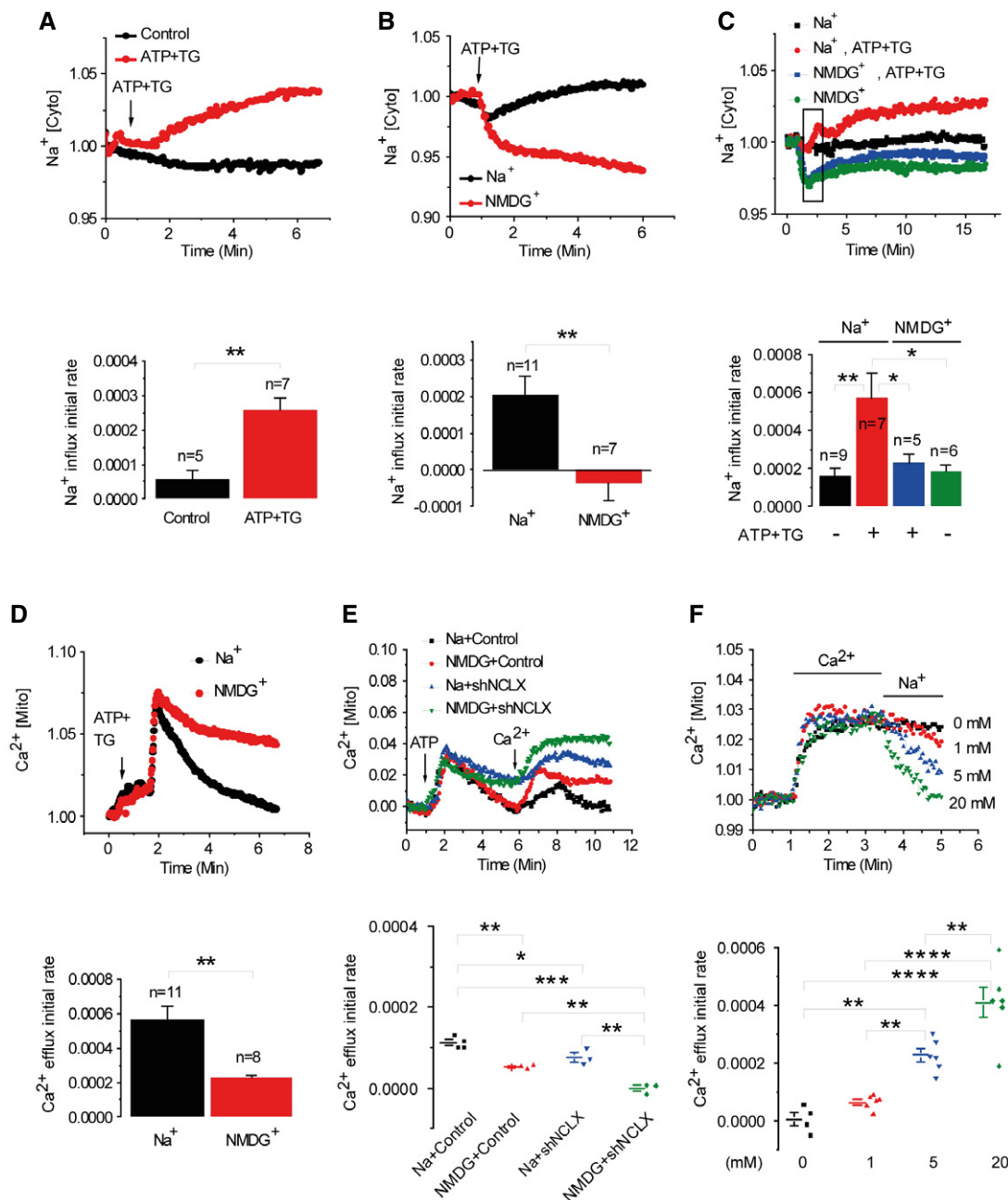


**Figure 6. Depletion of intracellular Ca<sup>2+</sup> stores triggers cytosolic Na<sup>+</sup> influx which drives NCLX-associated mitochondrial Na<sup>+</sup> influx and Ca<sup>2+</sup> efflux.**

- A Upper panel: Fluorescence traces of cytosolic Na<sup>+</sup> responses, Na<sup>+</sup> [Cyto], in ATP-depleted cells (n = 7) versus control non-depleted HEK293T cells (n = 5) loaded with Asanta Natrium. Na<sup>+</sup> influx averaged rates are shown in the lower panel.
- B Upper panel: Fluorescence traces of cytosolic Na<sup>+</sup>. Lower panel: Averaged rates of cytosolic Na<sup>+</sup> influx in cells superfused with either Na<sup>-</sup> (n = 11) or NMDG<sup>+</sup> (n = 7)-containing Ringer's solution.
- C Upper panel: Traces of mitochondrial Na<sup>+</sup> transport in cells preloaded with the mitochondrial Na<sup>+</sup> dye, CoroNa red in HEK293T cells. Lower panel: Mitochondrial Na<sup>+</sup> influx rates in the presence (n = 7) or absence (n = 5) of Na<sup>+</sup>.
- D Upper panel: Traces of mitochondrial Ca<sup>2+</sup>, Ca<sup>2+</sup> [Mito], recorded by monitoring RP-mt fluorescence following Ca<sup>2+</sup>-store depletion in HEK293T cells by ATP and TG as in Fig 1B in the presence of Na<sup>+</sup> or NMDG<sup>+</sup>. Lower panel: Mitochondrial Ca<sup>2+</sup> efflux in cells in the presence of NMDG<sup>+</sup> (n = 8) compared to Na<sup>+</sup> (n = 11).
- E Upper panel: Traces of Ca<sup>2+</sup> [Mito] of cell superfused with ATP alone in Ca<sup>2+</sup>-free Ringer followed by superfusion with Ca<sup>2+</sup> Ringer with or without Na<sup>+</sup> in shControl cells versus shNCLX cells. Lower panel: Rates of traces shown in the upper panel in the presence (n = 4) or absence (n = 3) of Na<sup>+</sup> ions in cells transfected with shControl (n = 3) or shNCLX (n = 3).
- F Upper panel: Cytosolic Na<sup>+</sup>-dose dependence of Ca<sup>2+</sup> [Mito] efflux. Lower panel: Mitochondrial Ca<sup>2+</sup> efflux rates at the indicated concentrations of Na<sup>+</sup> [mM] [0 (n = 4); 1, 5 and 20 (n = 6)].

Data information: The results are presented as the means ± SEM. \*P < 0.05; \*\*P < 0.01; \*\*\*P < 1E-03; \*\*\*\*P < 1E-04. P-values indicate the results of an unpaired Student's t-test (A, B and D) or one-way ANOVA test followed by Tukey *post hoc* analysis (C, E and F).

**Figure 7. Mitochondrial catalase (m-catalase) rescues SOCE, CRAC, and mitochondrial redox responses after NCLX knockdown.**

- A Upper panel: Traces of mitochondrial roGFP1 fluorescence in HEK293T cells co-transfected with either siControl or siNCLX and  $\text{Ca}^{2+}$ -store depleted as described in Fig 1B. Changes in roGFP1 410/480 ratio fluorescence were determined using minimal and maximal values obtained by application of 100 mM DTT and 10 mM  $\text{H}_2\text{O}_2$ , respectively, as described in Materials and Methods. Lower panel:  $\Delta F$  ratio of redox change after  $\text{Ca}^{2+}$  restoration to the external milieu in siControl cells ( $n = 8$ ) compared to siNCLX cells ( $n = 12$ ).
- B Upper panel: Effect of NCLX on redox state determined by monitoring NAD(P)H intrinsic fluorescence in HEK293T cells, transfected with either siNCLX or siControl, and treated as described in Fig 1B. Oligomycin or FCCP were used for calibration and added where indicated. Lower panel: Averaged autofluorescence rates after adding Ringer's solution containing  $\text{Ca}^{2+}$ .
- C Upper panel: Effect of mitochondrial catalase (pZeoSV2 + mCat) expression. Lower panel: Rates of redox change in siNCLX + pZeoSV2 + (pZeo) empty vector transfected cells ( $n = 4$ ) compared to siNCLX cells transfected with m-catalase ( $n = 6$ ).
- D Upper panel: Fluorescence traces of cytosolic  $\text{Ca}^{2+}$  responses in HEK293T cells co-transfected with either siControl or siNCLX together with pZeo or m-catalase. Lower panel: Averaged rates of  $\text{Ca}^{2+}$  influx in cells transfected with siNCLX ( $n = 9$ ) or cells co-transfected with siNCLX and either m-catalase ( $n = 9$ ) or pZeo ( $n = 5$ ) compared to cells transfected with siControl ( $n = 6$ ) or co-transfected with siControl and m-catalase ( $n = 5$ ).
- E–H CRAC electrophysiological recordings in HEK293T cells activated by dialysis of 20 mM BAPTA through the patch pipette under the same conditions of transfection used in (B). I–V relationships are shown in (G) and statistical analysis on  $\text{Na}^+$  CRAC currents measured at  $-100$  mV is shown in (H). m-Catalase is routinely co-transfected with a plasmid encoding eGFP for identification of transfected cells.

Data information: The results are presented as the means  $\pm$  SEM. \* $P < 0.05$ ; \*\* $P < 0.01$  \*\*\* $P < 1E-03$ .  $P$ -values indicate the results of an unpaired Student's  $t$ -test (A–C) or one-way ANOVA test followed by Tukey *post hoc* analysis (D–H).

expression was followed by a strong inhibition of CRAC current (Fig 7E–H). Remarkably, targeting catalase to the mitochondria was sufficient to rescue CRAC currents in cells in which NCLX was knocked down (Fig 7F and H). We compared the basal redox state of siNCLX cells vs siNCLX cells expressing m-catalase and found that siNCLX cells are slightly more oxidized, although this difference was not significant (Fig EV5C). Together, our results strongly support a novel paradigm whereby NCLX control of the mitochondrial redox state participates in mitochondrial communication with SOCE.

Since our results (Fig 2) indicate that the NCLX effect on SOCE is not mediated via disruption of STIM1 and Orai1 interactions, we reasoned that the mitochondrial redox response evoked by NCLX is targeting a redox-sensitive residue on Orai1. Orai1 possesses three cysteine residues potentially modified by oxidants, Cys126, Cys143, and Cys195. One of the Orai1 cysteine residues, Cys195, has recently emerged as a redox responsive element within this channel (Bogeski *et al*, 2010). We therefore focused on Cys195 within Orai1 and compared the wild-type SOCE response (Fig 8A) to the SOCE response of either Orai1 or Orai1 C195S coexpressed with STIM1 in either siControl- or siNCLX-transfected HEK293T cells (Fig 8B and C). Remarkably, while the silencing of NCLX was followed by reduction in native as well overexpressed Orai1-dependent  $\text{Ca}^{2+}$  influx, mutating Cys195 to serine (C195S) fully rescued Orai1-dependent SOCE in NCLX knockdown cells (Fig 8C). To establish the role of this residue in mediating the NCLX-dependent redox effect on Orai1, we analyzed Orai1-mediated CRAC currents in HEK293T cells expressing STIM1 with either Orai1 or the Orai1-C195S mutant (Fig 8D–I) while depleting internal stores and strongly buffering cytosolic  $\text{Ca}^{2+}$  with 20 mM BAPTA, as defined in Fig 1. Consistent with data obtained with SOCE measurements using Fura-2, the inhibitory effect of NCLX knockdown was also observed on CRAC currents in cells over-expressing STIM1 and Orai1. In contrast, mutating the redox-sensitive cysteine 195 to serine (C195S) fully rescued Orai1-mediated CRAC currents following the knockdown of NCLX. Mutation of all three cysteines Cys126, Cys143, and Cys195 in Orai1 to serine also fully rescued Orai1-mediated CRAC currents following the knockdown of NCLX (Fig 8J–L). CRAC currents mediated by this triple Orai1 mutant were significantly bigger than those mediated by either Orai1 or

Orai1-C195S (Orai1; 17.62, C195S-Orai1; 16.52, C126S/C143S/C195S-Orai1; 51.59). Taken together, our results indicate that the mitochondrial redox transients controlled by NCLX prevent CRAC channel inhibition mediated by oxidation of cysteine 195 on Orai1.

## Discussion

Although a role for mitochondrial  $\text{Ca}^{2+}$  signaling in regulating SOCE is well established, the mode of communication between these two domains is not understood. The recent identification of the mitochondrial  $\text{Ca}^{2+}$  transporters enables more selective molecular tools to specifically control their activity and study their role in controlling SOCE. In this study, we have focused on NCLX whose rate of mitochondrial  $\text{Ca}^{2+}$  removal is two orders of magnitude slower than the mitochondrial  $\text{Ca}^{2+}$  influx. Thus, NCLX is the rate limiting component in mitochondrial  $\text{Ca}^{2+}$  shuttling. NCLX is also a  $\text{Na}^+$  transporter that mediates the exchange of 3  $\text{Na}^+$  per 1  $\text{Ca}^{2+}$  making it the major mitochondrial  $\text{Na}^+$  uptake pathway (Baysal *et al*, 1994; Jung *et al*, 1995).  $\text{Na}^+$  transport was previously linked to SOCE. Thus, it was proposed that  $\text{Na}^+$  influx occurs through concomitant activation of non-selective TRPC cation channels in response to pharmacological or receptor-mediated store depletion (Parekh & Putney, 2005). However, the role of cytosolic  $\text{Na}^+$  in regulating the highly  $\text{Ca}^{2+}$  selective Orai1 channel is still poorly understood. In this study, we sought to address the following questions. Does NCLX control SOCE-dependent  $\text{Ca}^{2+}$  signaling? And, if so, what is the mechanism of NCLX-mediated regulation of SOCE? Our results indicate that NCLX is required for SOCE and support a redox effect of NCLX on CRAC channels that is independent of mitochondrial  $\text{Ca}^{2+}$  buffering.

An important mode of cross talk between CRAC channels and mitochondria is based on the ability of mitochondria to control  $\text{Ca}^{2+}$  concentrations at the vicinity of the CRAC channel thereby decreasing their  $\text{Ca}^{2+}$ -dependent inactivation. Such interaction between the mitochondria and CRAC channels is particularly prominent in immune cells (Rizzuto *et al*, 1998, 2012; Alvarez *et al*, 1999; Berridge *et al*, 2003; Singaravelu *et al*, 2011), in which inhibition of MCU and, more recently, molecular knockdown of MCU have

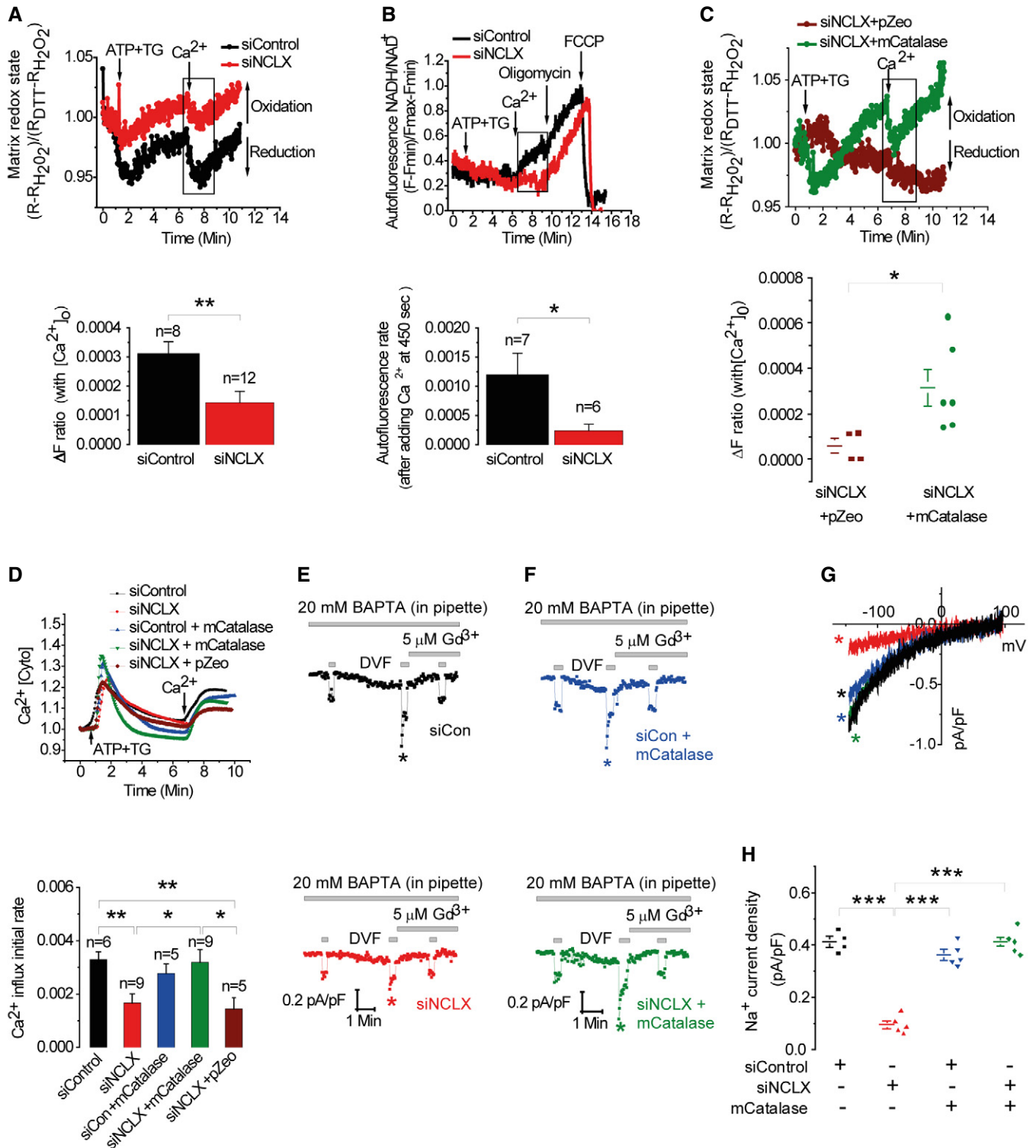
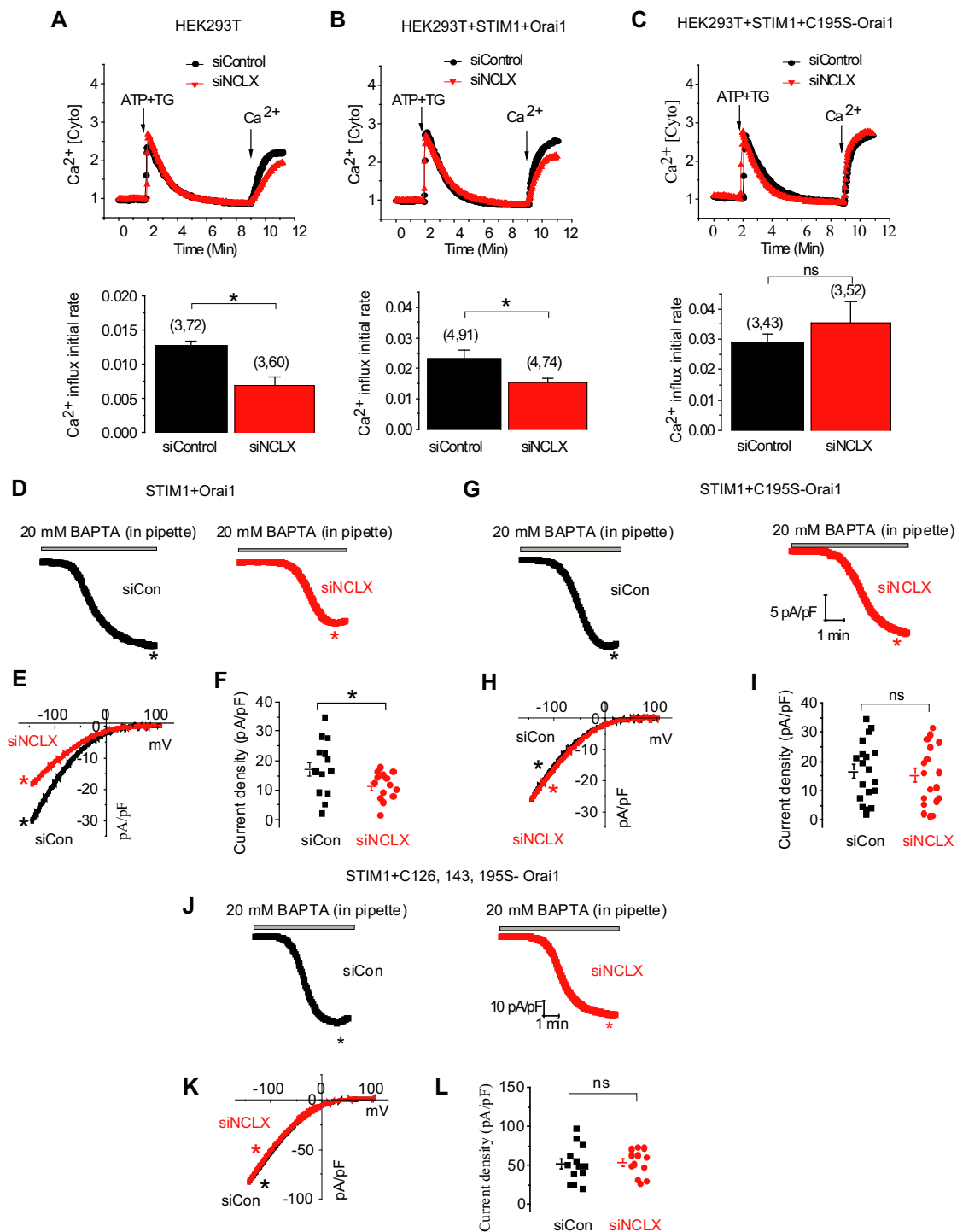


Figure 7.

demonstrated that SOCE is inhibited by the block of mitochondrial  $Ca^{2+}$  uptake in immune cells (Gilabert *et al*, 2001; Ma & Beaven, 2011). In other cell types, however, the proximity of the mitochondria to CRAC channels is less pronounced (Naghdi *et al*, 2010). Studies employing organellar  $Ca^{2+}$  reporters targeted, for example, to the outer mitochondrial membrane and the plasma membrane

suggest that mitochondria are not mediating strong  $Ca^{2+}$  changes at the vicinity of the CRAC channel (Giacomello *et al*, 2010). Furthermore, inhibition of mitochondrial efflux by the NCLX inhibitor CGP-37157b enhances mitochondrial  $Ca^{2+}$  uptake rather than decreasing it and yet leads to similar inhibition of SOCE. These findings indicate that in addition to the  $Ca^{2+}$ -dependent inactivation, there is an



**Figure 8. C195S mutation in Orai1 prevents the inhibitory effect of SOCE and CRAC current caused by NCLX knockdown.**

A–C HEK293T cells were transfected with either control siRNA (black) or NCLX siRNA (red) and incubated for 72 h (A). Cells were then transfected again with siRNA along with either plasmids, STIM1 and Orai1 (B), or plasmids, STIM1 and C195S-Orai1 (C), and incubated for another 24 h. The numbers in bar graphs (i.e., (x, y)) represent the total number of independent recording (x) and the total number of cells from all recordings (y). SOCE was triggered as described in Fig 1B, and Fura-2 fluorescence was monitored as described in Materials and Methods. Averaged rates of  $Ca^{2+}$  influx were shown in the lower panels.

D–L Representative time course traces (D and G) of Orai1- and Orai1-C195S-mediated CRAC currents activated by dialysis through the patch pipette of a solution containing 20 mM BAPTA and recorded in a bath solution containing 20 mM  $Ca^{2+}$ . I–V curves are shown in (E and H) which are taken from traces as indicated by color-coded asterisks. Scatter blots (F and I) depict maximal CRAC currents values taken at –100 mV and represented as current densities (pA/pF). Similar CRAC current recordings from HEK293T cells expressing STIM1 and C126S/C143S/C195S-Orai1 triple mutant are shown in (J–L).

Data information: The results are presented as the means  $\pm$  SEM. \* $P < 0.05$ ; ns, not significant.  $P$ -values indicate the results of an unpaired Student's  $t$ -test.







(Carafoli *et al*, 1974; Palty *et al*, 2004). The latter finding also provides strong evidence for a distinct role of NCLX in the regulation of CRAC currents because plasma membrane NCX members are inert to  $\text{Li}^+$ . However, it is important to note that the reverse mode of the plasma membrane NCX triggered by a SOCE-associated  $\text{Na}^+$  rise (e.g. through TRPC6) is also contributing to cytosolic  $\text{Ca}^{2+}$  rise (Borin *et al*, 1993; Lemos *et al*, 2007, 2007). Unlike NCLX, the NCX effect on cytosolic  $\text{Ca}^{2+}$  is not mediated through direct action on CRAC conductance. Therefore, our current and previous studies (Borin *et al*, 1993; Lemos *et al*, 2007; Nita *et al*, 2014a,b) indicate that NCLX and NCX concertedly amplify SOCE-dependent cytosolic  $\text{Ca}^{2+}$  signals but through different mechanisms. For NCX, the SOCE-dependent  $\text{Na}^+$  rise triggers its reverse mode leading to increased cytosolic  $\text{Ca}^{2+}$  while for NCLX it triggers forward activation that can lead to maintenance of CRAC channel activity (Fig 9). How does the powering of NCLX by cytosolic  $\text{Na}^+$  culminate in the activation of SOCE and CRAC currents? Mitochondria are not only the metabolic engine and a major hub for  $\text{Ca}^{2+}$  signaling, they function as major regulators of cellular redox potential (Szabadkai & Duchon, 2008; Nunes & Demaurex, 2014) that link between activation of NCLX to SOCE and CRAC currents.

Our results indicate that NCLX regulation of SOCE persists following the knockdown of MCU. Although the reason for this observation is not entirely clear, it is important to note that mitochondrial  $\text{Ca}^{2+}$  transients initiated by MCU reflect only ~5% of the total mitochondrial  $\text{Ca}^{2+}$ . The rest, ~95% of the mitochondrial  $\text{Ca}^{2+}$  pool, is an insoluble/soluble pool consisting mainly of the phosphate  $\text{Ca}^{2+}$  salt. The solubility of the latter pool is strongly pH dependent and therefore any change with matrix pH; for example, metabolic activity will trigger a matrix-free  $\text{Ca}^{2+}$  change and thereby a change in mitochondrial redox. Affinity and sensitivity of the mitochondrial  $\text{Ca}^{2+}$  sensitive dyes are, however, less than optimal (Pizzo *et al*, 2012). Therefore, these changes are often left unnoticed. Consistent with this hypothesis, our previous and current results show that the apparent duration of mitochondrial  $\text{Na}^+$  fluxes (which in contrast to  $\text{Ca}^{2+}$  is unbuffered) is much longer than mitochondrial  $\text{Ca}^{2+}$  transients (Palty *et al*, 2010; Nita *et al*, 2014a), indicating that NCLX is pumping out  $\text{Ca}^{2+}$  for much more extensive periods than the “apparent” mitochondrial  $\text{Ca}^{2+}$  transients. Finally, in contrast to MCU, NCLX is dually linked to  $\text{Ca}^{2+}$  and  $\text{Na}^+$  signaling which we show here is critical for redox regulation and the SOCE response.

Regulation by redox has recently emerged as a critical mode of SOCE regulation (Bogeski *et al*, 2010; Hawkins *et al*, 2010; Nunes & Demaurex, 2014).

There are several studies which show regulation of m-catalase (Nazioglu, 2012; Littlejohns *et al*, 2014). However, the  $\text{H}_2\text{O}_2$  clearing rate of catalase is mainly dependent on the levels of expression of catalase (Rodriguez *et al*, 2000). Therefore, over-expressed catalase targeted to the mitochondria (as described here) is expected to enhance  $\text{H}_2\text{O}_2$  detoxification in the mitochondria generated by abnormal mitochondrial  $\text{Ca}^{2+}$  rise.

Our previous results indicate that expression and activity of NCLX are critical in triggering a mitochondrial redox signal (De Marchi *et al*, 2014). Our current results demonstrating that catalase rescues the mitochondrial redox response and CRAC/SOCE in NCLX-deficient cells, suggest that diffusible  $\text{H}_2\text{O}_2$  is the link between NCLX and SOCE (Fig 9). While buffering of cytosolic  $\text{Ca}^{2+}$  failed to rescue SOCE and CRAC currents in NCLX knockdown cells, expression of

mitochondrial catalase leads to a full rescue of SOCE in NCLX knockdown cells. It may be argued that this effect is indirect and associated, for example, with ER  $\text{Ca}^{2+}$  release. However, our electrophysiological analysis in cells expressing the mitochondrial catalase also show rescue of CRAC currents. Redox potential is a key regulator of SOCE that can act on multiple targets in this pathway. The oligomerization of STIM1 and its interaction with Orai1 are redox-sensitive. However, our results indicate that the oligomerization of STIM1 and its interaction with Orai1 (as well as their expression) are not affected by knockdown of NCLX, arguing against such a scenario. Instead, our results suggest that the target of the mitochondrial redox response is an Orai1 cysteine residue (Cys195). Oxidation of the latter by  $\text{H}_2\text{O}_2$ , leads to CRAC channel inhibition (Bogeski *et al*, 2010). Furthermore, our finding showing that substitution of cysteine 195 in Orai1 with serine (C195S) is sufficient to rescue SOCE and CRAC currents indicate that redox-dependent regulation of SOCE by mitochondria is mediated through cysteine 195 of Orai1 (Fig 9).

In conclusion, the results of this study identify a long sought and novel mode of interaction between the mitochondria and SOCE. This pathway integrates  $\text{Na}^+$  and  $\text{Ca}^{2+}$  signals that converge on the mitochondrial NCLX  $\text{Na}^+/\text{Ca}^{2+}$  exchanger, to modulate cellular redox which controls SOCE and CRAC currents, mediated by a redox-sensitive site on Orai1 (Fig 9).

## Materials and Methods

### Cell culture and transfection

HEK293T cells (human embryonic kidney cell line) were cultured in Dulbecco's modified Eagle's medium supplemented with 10% fetal calf serum, 1% penicillin/streptomycin, 2 mM L-glutamine. Transfection of HEK293T cells was performed using the  $\text{CaPO}_4$  precipitation protocol in cultures of 30–50% confluence, as previously described (Palty *et al*, 2004). Vascular smooth muscle cells (VSMCs) were cultured on glass coverslips and transfected with DharmaFECT 1 (Dharmacon, T-2001). siRNA NCLX or siControl was diluted in DharmaFECT siRNA transfection reagent, incubated ~20 min at room temperature and then added in the antibiotics-free media. The efficiency of transfection was assessed by visualizing Dharmacon siGLO Red (Dharmacon, D-001630-02-05) transfection particles according to the protocol provided by manufacturer. The transfection efficiency, for siNCLX delivery as determined by siGLO fluorescent marker was high, ~90%. VSMCs were isolated as previously described (Potier *et al*, 2009) and maintained in culture 45% DMEM and 45% Ham's F12 with 10% FBS supplemented with L-glutamine) at 37°C, 5%  $\text{CO}_2$ , and 100% humidity, passaged and used within 1–5 passages. Rat basophilic leukemia (RBL-2H3) mast cells were obtained from ATCC, cultured in EMEM with 2 mmol/l L-glutamine and 10% FBS and maintained in a 37°C, 5%  $\text{CO}_2$  humidified incubator as described previously (Abdullaev *et al*, 2008).

### Plasmid and siRNA preparation

Double-stranded siRNAs used to silence NCLX expression were obtained from Applied Biosystems as previously described (Palty *et al*, 2010). The human NCLX shRNA plasmid was obtained from Sigma (Mission TRC shRNA Target Set TRCN-5045). The shMCU

and shControl plasmids were a gift from Fabiana Perocchi (TRCN0000133861; Baughman *et al*, 2011). The membrane-targeted GCAMP5 was obtained from Addgene [pN1 Lck-GCaMP5G (Plasmid #34924)]. The RP-mt plasmid was provided by Atsushi Miyawaki (Wako, Japan; Nagai *et al*, 2001). The roGFP1 was kindly gifted by Roger Y. Tsien (UCSD; Dooley *et al*, 2004). The pZeoSV2+ mCat and pZeoSV2+ empty vector were provided by J. Andres Melendez (Albany, USA; McCarthy *et al*, 2013). The plasmid of eYFP-STIM1 was kindly gifted by Tobias Meyer; the plasmid of CFP-Orai1 was provided by James W. Putney; and the plasmids of C195S-Orai1-eGFP and C126S/C143S/C195S-Orai1-eGFP were constructed by Mohamed Trebak's laboratory. All those tagged or mutant of STIM1 and Orai1 plasmids are used for patch clamp experiments.

### Immunoblot analysis

Immunoblot was performed with 100  $\mu$ g of protein samples obtained from HEK293T cells transfected with either siControl or siNCLX. Detection for NCLX, STIM1, and Orai1 proteins was performed 96 h post-transfection using specific antibodies; HSC 70 loading control is also shown. Anti-NCLX polyclonal antibody was generated in our laboratory as previously described (Palty *et al*, 2010) while anti-STIM1 monoclonal antibody was from BD Biosciences, anti-Orai1 polyclonal antibody was from Alomone Labs, and anti-HSC 70 was from Santa Cruz Biotechnology.

### Fluorescent Ca<sup>2+</sup> and Na<sup>+</sup> imaging

The imaging system consisted of an Axiovert 100 inverted microscope (Zeiss, Oberkochen, Germany), Polychrome V monochromator (Till Photonics, Planegg, Germany) and a Sensi-Cam cooled charge-coupled device (PCO, Kelheim, Germany). Fluorescence images were acquired with Imaging WorkBench 6.0 software (Axon Instruments, Foster City, CA, USA). Ca<sup>2+</sup> imaging was performed in HEK293T and VSMCs cells that were attached onto coverslips and superfused with Ringer's solution containing (in mM): 126 NaCl, 5.4 KCl, 0.8 MgCl<sub>2</sub>, 20 HEPES, 1.8 CaCl<sub>2</sub>, and 15 glucose; pH was adjusted to 7.4 with NaOH or NMDG<sup>+</sup> in Na<sup>+</sup>-free Ringer's solutions (Palty *et al*, 2010). For cytosolic Ca<sup>2+</sup> measurements, HEK293T and VSMCs cells were loaded with Fura-2 AM (2  $\mu$ M) for 25 min at room temperature or 4  $\mu$ M for 45 min at 37°C, respectively (Bisaillon *et al*, 2010). Cell were excited with 340/380 nm wavelength light and imaged using a 510-nm long-pass filter, as described previously (Jonkers & Henquin, 2001). For measurements of plasma membrane-localized Ca<sup>2+</sup> signals, HEK293T cells were transfected with 1  $\mu$ g of GCamp5 which is targeted solely to the plasma membrane. The membrane-targeted Gcamp5 was excited at 485 nm, and fluorescence was monitored at 510 nm emission (Akerboom *et al*, 2012). Mitochondrial Ca<sup>2+</sup> measurements were performed in HEK293T cells expressing ratio-metric mitochondrial pericam (mitopericam), which is targeted solely to the inner membrane of mitochondria. The mitochondrial pericam fluorescence in HEK293T cells was acquired at 430 nm excitation and 550 nm emission, as described previously (Nagai *et al*, 2001). Cytosolic Na<sup>+</sup> levels were recorded in Asanta Sodium Green-2 (Teflabs, Jackson Springs, NC, USA)-loaded HEK293T cells excited with 485 nm and imaged at 510-nm long-pass filter. It is well known that CoroNa Red is localized to the mitochondria (Yang *et al*, 2004; Baron *et al*, 2005; see in Appendix Fig S3). Therefore,

mitochondrial Na<sup>+</sup> signals were monitored in cells loaded with CoroNa Red (Molecular Probes) at excitation of 568 nm and emission at 590 nm, respectively (Lemos *et al*, 2007). Note that at 50 s, Na<sup>+</sup> fluorescence falls a bit. This change is apparent in the presence or absence of Na<sup>+</sup> and therefore a fluorescence artifact due to addition of solution.

For all single-cell imaging experiments, traces of averaged responses were analyzed and plotted using Origin Labs software. The fluorescent Na<sup>+</sup> or Ca<sup>2+</sup> signals were normalized once again to the averaged baseline signal ( $F/F_0$  or  $R/R_0$ ), obtained at the beginning of the measurements. The influx and efflux rates were derived from a linear fit of the fluorescence change during 30 s (Palty *et al*, 2010; Nita *et al*, 2012). Averaged rates of the fluorescent Na<sup>+</sup> or Ca<sup>2+</sup> responses, over  $n$  (indicated in the figure legends) experiments, are presented in the bar graphs and analyzed using Origin software.

### Mitochondrial redox state measurements

Ratiometric measurements of the mitochondrial redox state were performed on using the same instrument as described above using the mitochondrial targeted, genetically encoded sensor roGFP1. Cells were excited at 410 and 480 nm and emission was collected at 535 nm. Images were acquired every 2 s. The 410/480 fluorescence ratios were normalized by obtaining the maximum and minimum ratios (obtained after addition of 1 mM H<sub>2</sub>O<sub>2</sub> and of 10 mM DTT, respectively; De Marchi *et al*, 2014). The fluorescence signals of roGFP1 were normalized to the averaged baseline signal ( $F/F_0$  or  $R/R_0$ ), obtained at the beginning of the measurements.

### Measurements of NADH fluorescence

NAD(P)H intrinsic fluorescence in HEK293T cells was fluorescently monitored (360 nm excitation and 440 nm emission) in an inverted microscope (see Fluorescent Ca<sup>2+</sup> and Na<sup>+</sup> imaging), as previously reported (Nita *et al*, 2012) and calibrated by superfusing the cell with a Ringer's solution containing 2  $\mu$ M FCCP, protonophore carbonyl cyanide 4-(trifluoromethoxy)phenylhydrazone (Ascent Laboratories, Asc-081) and 1  $\mu$ M oligomycin (Merck Millipore, MBS495455) at the end of the experiments.

### Confocal microscopy

HEK293T cells were grown onto six-well chamber slides (Nunc, Rochester, NY, U.S.A.) and transfected with membrane-targeted GCamp5 (0.2  $\mu$ g of DNA/well). Forty-eight hours following transfection, samples were examined by fluorescence confocal microscopy (LSM510 system, Carl Zeiss, Jena, Germany) using 480 nm (Ca<sup>2+</sup> insensitive) excitation laser and 505-nm long-pass emission filter as previously described (Feldman *et al*, 2010). Briefly, baseline picture was captured followed by incubation with 2  $\mu$ M of thapsigargin (TG) for 3 min. Then, cells were perfused by Ringer's solution containing 5 mM of CaCl<sub>2</sub> before starting recordings.

### Föster resonance energy transfer measurements

These measurements were done as described previously (Navarro-Borelly *et al*, 2008; Wang *et al*, 2014; Zhou *et al*, 2015; Cai *et al*, 2016). To determine resonance energy transfer (FRET) signals

between Orai1-CFP and STIM1-YFP, we used the Leica DMI 6000B fluorescence microscope equipped with CFP (438Ex/483Em), YFP (500Ex/542Em), FRET (438Ex/542Em) filters. Fluorescence intensities captured with the CFP, YFP, and FRET filters were collected at room temperature using a 40 $\times$  oil objective (N.A.1.35; Leica) and processed using Slidebook 6.0 software (Intelligent Imaging Innovations). Three-channel corrected FRET was calculated using the following formula:  $F_C = I_{DA} - Fd/Dd * I_{DD} - Fa/Da * I_{AA}$ , where  $I_{DD}$ ,  $I_{AA}$ , and  $I_{DA}$  represent the background-subtracted CFP, YFP, and FRET images, respectively. And  $F_C$  represents the corrected energy transfer,  $Fd/Dd$  represents measured bleed-through of CFP through the FRET filter (0.457), and  $Fa/Da$  is measured bleed-through of YFP through the FRET filter (0.19). Although the CFP signal was constant in Orai1-CFP stable cells, there was some variation in transiently expressed STIM1-YFP levels. To minimize the variation, only cells with similar YFP intensity were analyzed. Also, the above FRET values were normalized against acceptor fluorescence (FYFP) to generate normalized FRET signals, which compensated for these variations in YFP expression. Thus, normalized FRET (NFRET) =  $FRET_C/I_{AA}$ . Average FRET measurements shown are typical of at least three independent analyses  $\pm$  SEM. Same data pool was also calculated for EFRET with following formula (Zal & Gascoigne, 2004):  $E_{app} = F_C / (F_C + G * I_{DD})$ , where the  $F_C = I_{DA} - Fd/Dd * I_{DD} - Fa/Da * I_{AA}$ .  $G$  is the instrument-specific constant and was determined as described (Zal & Gascoigne, 2004; Navarro-Borelly et al, 2008).  $G$  value is  $1.9 \pm 0.1$  ( $n = 32$  cells). Only cells with similar YFP/CFP ratio were used for EFRET analysis.

### Patch clamp electrophysiology

Conventional whole-cell patch clamp recordings were carried out using an Axopatch 200B and Digidata 1440A (Molecular Devices, LLC, Sunnyvale, CA) as previously published (Gonzalez-Cobos et al, 2013; Zhang et al, 2013, 2014). Pipettes were pulled from borosilicate glass capillaries (World Precision Instruments, Inc., Sarasota, FL) with a P-97 flaming/brown micropipette puller (Sutter Instrument Company, Novato, CA) and polished with DMF1000 (World Precision Instruments). Resistances of filled glass pipettes were 2–4 M $\Omega$ . Series resistances were < 10 M $\Omega$ . The liquid-junction potential offset was around 5 mV and was corrected. Only cells with tight seals (> 13 G $\Omega$ ) were selected for break-in. Cells were maintained at a 0 mV holding potential during experiments and subjected to voltage ramps from –140 to +100 mV lasting 250 ms every 2 s. All experiments were performed at room temperature (20–25°C). Clampfit 10.1 software was used for data analysis. The solutions employed for patch clamp recordings are as follows.

#### Bath solution

115 mM Na<sup>+</sup>-methanesulfonate, 10 mM CsCl, 1.2 mM MgSO<sub>4</sub>, 10 mM HEPES, 20 mM CaCl<sub>2</sub>, and 10 mM glucose (pH was adjusted to 7.4 with NaOH). For Li<sup>+</sup> based bath, we replaced Na<sup>+</sup>-methanesulfonate with Li<sup>+</sup>-methanesulfonate; for N-methyl-D-glutamine (NMDG<sup>+</sup>)-based bath, we replaced Na<sup>+</sup>-methanesulfonate with NMDG<sup>+</sup>.

#### Pipette solution (20 mM BAPTA)

115 mM Cs-methanesulfonate, 20 mM Cs-1,2-bis-(2-aminophenoxy) ethane-N,N,N',N'-tetraacetic acid (Cs-BAPTA), 8 mM MgCl<sub>2</sub>, and

10 mM HEPES (pH adjusted to 7.2 with CsOH). For high buffer, we replaced 20 mM Cs-BAPTA with 50 mM in pipette solution.

#### Pipette solution (0.1 mM EGTA)

135 mM Cs<sup>+</sup>-methanesulfonate, 8 mM NaCl, 1.0 mM MgCl<sub>2</sub>, 0.1 mM EGTA, and 10 mM HEPES, 0.03 mM IP<sub>3</sub> (pH adjusted to 7.2 with CsOH). For cocktail, we added 2 mM pyruvic acid, 2 mM malic acid, 1 mM NaH<sub>2</sub>PO<sub>4</sub>, 0.5 mM cAMP, 2 mM ATP, 0.5 mM GTP to the pipette solution.

To energize the mitochondria a pipette solution containing a cocktail (2 mM pyruvic acid, 2 mM malic acid, 1 mM NaH<sub>2</sub>PO<sub>4</sub>, 0.5 mM cAMP, 0.5 mM GTP, 0.5 mM MgCl<sub>2</sub>) was used. Note, that the mitochondria also led to enhanced CRAC current only when activated in the presence of weak to moderate concentrations of EGTA (< 0.6 mM EGTA; Gilabert & Parekh, 2000; Parekh, 2008), presumably through enhanced mitochondrial Ca<sup>2+</sup> buffering and reduced Ca<sup>2+</sup>-dependent negative feedback on CRAC channels. When indicated, we performed CRAC recordings using a pipette solution containing 0.1 mM of the chelator EGTA combined with IP<sub>3</sub>.

#### Divalent-free (DVF) bath solution

155 mM Na-methanesulfonate, 10 mM HEDTA, 1 mM EDTA, and 10 mM HEPES (pH 7.4, adjusted with NaOH).

### Statistical analysis

The results of the experiments are presented as the means  $\pm$  SEM of  $\geq 4$  experiments ( $n$ ), using 5–30 cells in each condition. Statistical significance for all experiments was determined using either unpaired two-tailed Student's *t*-test or one-way ANOVA test followed by Tukey *post hoc* analysis. Values of  $P < 0.05$  were considered significant.

**Expanded View** for this article is available online.

### Acknowledgements

This study was funded by the DIP and ISF grants to IS and MH and by grants R21AG050072, R01HL097111 and R01HL123364 from the NIH and by the American Heart Association grant 14GRNT18880008 and Qatar National Research Fund (QNRF) grant # NPRP8-110-3-021 to M.T. We wish to thank Dr. J. Andres Melendez (SUNY Albany) for the generous gift of the m-catalase construct and Dr. Iulia Nita for helping with the NAD(P)H experiments.

### Author contributions

IS, MT, TBKN, XZ, and DLG wrote the manuscript; TBKN, XZ, AE, SR, YZ, RKM, and MG performed the experiments; JAS, NH, MH, DLG, MT, and IS provided experimental oversight. IS, MT, TBKN, XZ, and AE designed the experiments; IS, MT, TBKN, XZ, MH, and DLG interpreted the data.

### Conflict of interest

The authors declare that they have no conflict of interest.

### References

Abdullaev IF, Bisailon JM, Potier M, Gonzalez JC, Motiani RK, Trebak M (2008) Stim1 and Orai1 mediate CRAC currents and store-operated

- calcium entry important for endothelial cell proliferation. *Circ Res* 103: 1289–1299
- Akerboom J, Chen TW, Wardill TJ, Tian L, Marvin JS, Mutlu S, Calderon NC, Esposti F, Borghuis BG, Sun XR, Gordus A, Orger MB, Portugues R, Engert F, Macklin JJ, Filosa A, Aggarwal A, Kerr RA, Takagi R, Kracun S et al (2012) Optimization of a GCaMP calcium indicator for neural activity imaging. *J Neurosci* 32: 13819–13840
- Alvarez J, Montero M, Garcia-Sancho J (1999) Subcellular Ca<sup>2+</sup> dynamics. *News Physiol Sci* 14: 161–168
- Ardon F, Rodriguez-Miranda E, Beltran C, Hernandez-Cruz A, Darszon A (2009) Mitochondrial inhibitors activate influx of external Ca<sup>2+</sup> in sea urchin sperm. *Biochim Biophys Acta* 1787: 15–24
- Baron S, Caplanusi A, van de Ven M, Radu M, Despa S, Lambrichts I, Ameloot M, Steels P, Smets I (2005) Role of mitochondrial Na<sup>+</sup> concentration, measured by CoroNa red, in the protection of metabolically inhibited MDCK cells. *J Am Soc Nephrol* 16: 3490–3497
- Baryshnikov SG, Pulina MV, Zulian A, Linde CI, Golovina VA (2009) Orai1, a critical component of store-operated Ca<sup>2+</sup> entry, is functionally associated with Na<sup>+</sup>/Ca<sup>2+</sup> exchanger and plasma membrane Ca<sup>2+</sup> pump in proliferating human arterial myocytes. *Am J Physiol Cell Physiol* 297: C1103–C1112
- Baughman JM, Peroochi F, Girgis HS, Plovanih M, Belcher-Timme CA, Sancak Y, Bao XR, Strittmatter L, Goldberger O, Bogorad RL, Koteliansky V, Mootha VK (2011) Integrative genomics identifies MCU as an essential component of the mitochondrial calcium uniporter. *Nature* 476: 341–345
- Baysal K, Jung DW, Gunter KK, Gunter TE, Brierley GP (1994) Na(+)-dependent Ca<sup>2+</sup> efflux mechanism of heart mitochondria is not a passive Ca<sup>2+</sup>/2Na<sup>+</sup> exchanger. *Am J Physiol* 266: C800–C808
- Berridge MJ, Bootman MD, Roderick HL (2003) Calcium signalling: dynamics, homeostasis and remodelling. *Nat Rev Mol Cell Biol* 4: 517–529
- Bers DM, Barry WH, Despa S (2003) Intracellular Na<sup>+</sup> regulation in cardiac myocytes. *Cardiovasc Res* 57: 897–912
- Bisaillon JM, Motiani RK, Gonzalez-Cobos JC, Potier M, Halligan KE, Alzawahra WF, Barroso M, Singer HA, Jourdeheuil D, Trebak M (2010) Essential role for STIM1/Orai1-mediated calcium influx in PDGF-induced smooth muscle migration. *Am J Physiol Cell Physiol* 298: C993–C1005
- Bogeski I, Kummerow C, Al-Ansary D, Schwarz EC, Koehler R, Kozai D, Takahashi N, Peinelt C, Griesemer D, Bozem M, Mori Y, Hoth M, Niemeyer BA (2010) Differential redox regulation of ORAI ion channels: a mechanism to tune cellular calcium signaling. *Sci Signal* 3: ra24
- Borin ML, Goldman WF, Blaustein MP (1993) Intracellular free Na<sup>+</sup> in resting and activated A7r5 vascular smooth muscle cells. *Am J Physiol* 264: C1513–C1524
- Cai X, Zhou Y, Nwokonko RM, Loktionova NA, Wang X, Xin P, Trebak M, Wang Y, Gill DL (2016) The orai1 store-operated calcium channel functions as a hexamer. *J Biol Chem* 291: 25764–25775
- Carafoli E, Tiozzo R, Lugli G, Crovetto F, Kratzing C (1974) The release of calcium from heart mitochondria by sodium. *J Mol Cell Cardiol* 6: 361–371
- De Marchi U, Santo-Domingo J, Castelbou C, Sekler I, Wiederkehr A, Demaurex N (2014) NCLX protein, but not LETM1, mediates mitochondrial Ca<sup>2+</sup> extrusion, thereby limiting Ca<sup>2+</sup>-induced NAD(P)H production and modulating matrix redox state. *J Biol Chem* 289: 20377–20385
- De Stefani D, Raffaello A, Teardo E, Szabo I, Rizzuto R (2011) A forty-kilodalton protein of the inner membrane is the mitochondrial calcium uniporter. *Nature* 476: 336–340
- Deak AT, Blass S, Khan MJ, Groschner LN, Waldeck-Weiermair M, Hallstrom S, Graier WF, Malli R (2014) IP3-mediated STIM1 oligomerization requires intact mitochondrial Ca<sup>2+</sup> uptake. *J Cell Sci* 127: 2944–2955
- Demaurex N, Poburko D, Frieden M (2009) Regulation of plasma membrane calcium fluxes by mitochondria. *Biochim Biophys Acta* 1787: 1383–1394
- Dooley CT, Dore TM, Hanson GT, Jackson WC, Remington SJ, Tsien RY (2004) Imaging dynamic redox changes in mammalian cells with green fluorescent protein indicators. *J Biol Chem* 279: 22284–22293
- Eder P, Probst D, Rosker C, Poteser M, Wolinski H, Kohlwein SD, Romanin C, Groschner K (2007) Phospholipase C-dependent control of cardiac calcium homeostasis involves a TRPC3-NCX1 signaling complex. *Cardiovasc Res* 73: 111–119
- Feldman B, Fedida-Metula S, Nita J, Sekler I, Fishman D (2010) Coupling of mitochondria to store-operated Ca<sup>2+</sup>-signaling sustains constitutive activation of protein kinase B/Akt and augments survival of malignant melanoma cells. *Cell Calcium* 47: 525–537
- Feske S, Gwack Y, Prakriya M, Srikanth S, Puppel SH, Tanasa B, Hogan PG, Lewis RS, Daly M, Rao A (2006) A mutation in Orai1 causes immune deficiency by abrogating CRAC channel function. *Nature* 441: 179–185
- Giacomello M, Drago I, Bortolozzi M, Scorsetto M, Gianelle A, Pizzo P, Pozzan T (2010) Ca<sup>2+</sup> hot spots on the mitochondrial surface are generated by Ca<sup>2+</sup> mobilization from stores, but not by activation of store-operated Ca<sup>2+</sup> channels. *Mol Cell* 38: 280–290
- Gilbert JA, Parekh AB (2000) Respiring mitochondria determine the pattern of activation and inactivation of the store-operated Ca<sup>2+</sup> current I(CRAC). *EMBO J* 19: 6401–6407
- Gilbert JA, Bakowski D, Parekh AB (2001) Energized mitochondria increase the dynamic range over which inositol 1,4,5-trisphosphate activates store-operated calcium influx. *EMBO J* 20: 2672–2679
- Glitsch MD, Bakowski D, Parekh AB (2002) Store-operated Ca<sup>2+</sup> entry depends on mitochondrial Ca<sup>2+</sup> uptake. *EMBO J* 21: 6744–6754
- Gonzalez-Cobos JC, Zhang X, Zhang W, Ruhle B, Motiani RK, Schindl R, Muik M, Spinelli AM, Bisaillon JM, Shinde AV, Fahrner M, Singer HA, Matrougui K, Barroso M, Romanin C, Trebak M (2013) Store-independent Orai1/3 channels activated by intracrine leukotriene C4: role in neointimal hyperplasia. *Circ Res* 112: 1013–1025
- Hawkins BJ, Irrinki KM, Mallilankaraman K, Lien YC, Wang Y, Bhanumathy CD, Subbiah R, Ritchie MF, Soboloff J, Baba Y, Kurosaki T, Joseph SK, Gill DL, Madesh M (2010) S-glutathionylation activates STIM1 and alters mitochondrial homeostasis. *J Cell Biol* 190: 391–405
- He C, O'Halloran DM (2014) Analysis of the Na<sup>+</sup>/Ca<sup>2+</sup> exchanger gene family within the phylum Nematoda. *PLoS ONE* 9: e112841
- Hoth M, Fanger CM, Lewis RS (1997) Mitochondrial regulation of store-operated calcium signaling in T lymphocytes. *J Cell Biol* 137: 633–648
- Jayaraman S, Joo NS, Reitz B, Wine JJ, Verkman AS (2001a) Submucosal gland secretions in airways from cystic fibrosis patients have normal [Na(+)] and pH but elevated viscosity. *Proc Natl Acad Sci USA* 98: 8119–8123
- Jayaraman S, Song Y, Vetrivel L, Shankar L, Verkman AS (2001b) Noninvasive in vivo fluorescence measurement of airway-surface liquid depth, salt concentration, and pH. *J Clin Invest* 107: 317–324
- Jonkers FC, Henquin JC (2001) Measurements of cytoplasmic Ca<sup>2+</sup> in islet cell clusters show that glucose rapidly recruits beta-cells and gradually increases the individual cell response. *Diabetes* 50: 540–550
- Jung DW, Baysal K, Brierley GP (1995) The sodium-calcium antiport of heart mitochondria is not electroneutral. *J Biol Chem* 270: 672–678
- Lee KP, Yuan JP, So I, Worley PF, Muallem S (2010) STIM1-dependent and STIM1-independent function of transient receptor potential canonical (TRPC) channels tunes their store-operated mode. *J Biol Chem* 285: 38666–38673



- Lemos VS, Poburko D, Liao CH, Cole WC, van Breemen C (2007) Na<sup>+</sup> entry via TRPC6 causes Ca<sup>2+</sup> entry via NCX reversal in ATP stimulated smooth muscle cells. *Biochem Biophys Res Commun* 352: 130–134
- Liou J, Kim ML, Heo WD, Jones JT, Myers JW, Ferrell JE Jr, Meyer T (2005) STIM is a Ca<sup>2+</sup> sensor essential for Ca<sup>2+</sup>-store-depletion-triggered Ca<sup>2+</sup> influx. *Curr Biol* 15: 1235–1241
- Littlejohns B, Pasdois P, Duggan S, Bond AR, Heesom K, Jackson CL, Angelini GD, Halestrap AP, Suleiman MS (2014) Hearts from mice fed a non-obesogenic high-fat diet exhibit changes in their oxidative state, calcium and mitochondria in parallel with increased susceptibility to reperfusion injury. *PLoS ONE* 9: e100579
- Lytton J (2007) Na<sup>+</sup>/Ca<sup>2+</sup> exchangers: three mammalian gene families control Ca<sup>2+</sup> transport. *Biochem J* 406: 365–382
- Ma HT, Beaven MA (2011) Regulators of Ca<sup>2+</sup> signaling in mast cells: potential targets for treatment of mast cell-related diseases? *Adv Exp Med Biol* 716: 62–90
- Malli R, Frieden M, Osibow K, Zoratti C, Mayer M, Demaurex N, Graier WF (2003) Sustained Ca<sup>2+</sup> transfer across mitochondria is essential for mitochondrial Ca<sup>2+</sup> buffering, store-operated Ca<sup>2+</sup> entry, and Ca<sup>2+</sup> store refilling. *J Biol Chem* 278: 44769–44779
- McCarthy DA, Ranganathan A, Subbaram S, Flaherty NL, Patel N, Trebak M, Hempel N, Melendez JA (2013) Redox-control of the alarmin, Interleukin-1 $\alpha$ . *Redox Biol* 1: 218–225
- Nagai T, Sawano A, Park ES, Miyawaki A (2001) Circularly permuted green fluorescent proteins engineered to sense Ca<sup>2+</sup>. *Proc Natl Acad Sci USA* 98: 3197–3202
- Naghdi S, Waldeck-Weiermair M, Fertschai I, Poteser M, Graier WF, Malli R (2010) Mitochondrial Ca<sup>2+</sup> uptake and not mitochondrial motility is required for STIM1-Orai1-dependent store-operated Ca<sup>2+</sup> entry. *J Cell Sci* 123: 2553–2564
- Navarro-Borelly L, Somasundaram A, Yamashita M, Ren D, Miller RJ, Prakriya M (2008) STIM1-Orai1 interactions and Orai1 conformational changes revealed by live-cell FRET microscopy. *J Physiol* 586: 5383–5401
- Naziroglu M (2012) Molecular role of catalase on oxidative stress-induced Ca<sup>2+</sup> signaling and TRP cation channel activation in nervous system. *J Recept Signal Transduct Res* 32: 134–141
- Nita II, Hershinkel M, Fishman D, Ozeri E, Rutter GA, Sensi SL, Khananshvilii D, Lewis EC, Sekler I (2012) The mitochondrial Na<sup>+</sup>/Ca<sup>2+</sup> exchanger upregulates glucose dependent Ca<sup>2+</sup> signalling linked to insulin secretion. *PLoS ONE* 7: e46649
- Nita II, Hershinkel M, Kantor C, Rutter GA, Lewis EC, Sekler I (2014a) Pancreatic beta-cell Na<sup>+</sup> channels control global Ca<sup>2+</sup> signaling and oxidative metabolism by inducing Na<sup>+</sup> and Ca<sup>2+</sup> responses that are propagated into mitochondria. *FASEB J* 28: 3301–3312
- Nita II, Hershinkel M, Lewis EC, Sekler I (2014b) A crosstalk between Na channels, Na/K pump and mitochondrial Na transporters controls glucose-dependent cytosolic and mitochondrial Na signals. *Cell Calcium* 57: 69–75
- Nunes P, Demaurex N (2014) Redox regulation of store-operated Ca<sup>2+</sup> entry. *Antioxid Redox Signal* 21: 915–932
- Palty R, Ohana E, Hershinkel M, Volokita M, Elgazar V, Beharier O, Silverman WF, Argaman M, Sekler I (2004) Lithium-calcium exchange is mediated by a distinct potassium-independent sodium-calcium exchanger. *J Biol Chem* 279: 25234–25240
- Palty R, Silverman WF, Hershinkel M, Caporale T, Sensi SL, Parnis J, Nolte C, Fishman D, Shoshan-Barmatz V, Herrmann S, Khananshvilii D, Sekler I (2010) NCLX is an essential component of mitochondrial Na<sup>+</sup>/Ca<sup>2+</sup> exchange. *Proc Natl Acad Sci USA* 107: 436–441
- Parekh AB, Putney JW Jr (2005) Store-operated calcium channels. *Physiol Rev* 85: 757–810
- Parekh AB (2008) Mitochondrial regulation of store-operated CRAC channels. *Cell Calcium* 44: 6–13
- Patron M, Raffaello A, Granatiero V, Tosatto A, Merli G, De Stefani D, Wright L, Pallafacchina G, Terrin A, Mammucari C, Rizzuto R (2013) The mitochondrial calcium uniporter (MCU): molecular identity and physiological roles. *J Biol Chem* 288: 10750–10758
- Pitts BJ (1979) Stoichiometry of sodium-calcium exchange in cardiac sarcolemmal vesicles. Coupling to the sodium pump. *J Biol Chem* 254: 6232–6235
- Pizzo P, Drago I, Filadi R, Pozzan T (2012) Mitochondrial Ca<sup>2+</sup> homeostasis: mechanism, role, and tissue specificities. *Pflugers Archiv* 464: 3–17
- Poburko D, Liao CH, van Breemen C, Demaurex N (2009) Mitochondrial regulation of sarcoplasmic reticulum Ca<sup>2+</sup> content in vascular smooth muscle cells. *Circ Res* 104: 104–112
- Potier M, Trebak M (2008) New developments in the signaling mechanisms of the store-operated calcium entry pathway. *Pflugers Archiv* 457: 405–415
- Potier M, Gonzalez JC, Motiani RK, Abdullaev IF, Bisailon JM, Singer HA, Trebak M (2009) Evidence for STIM1- and Orai1-dependent store-operated calcium influx through ICRCAC in vascular smooth muscle cells: role in proliferation and migration. *FASEB J* 23: 2425–2437
- Putney JW Jr (1986) A model for receptor-regulated calcium entry. *Cell Calcium* 7: 1–12
- Reeves JP, Hale CC (1984) The stoichiometry of the cardiac sodium-calcium exchange system. *J Biol Chem* 259: 7733–7739
- Reyes RC, Verkhatsky A, Parpura V (2013) TRPC1-mediated Ca<sup>2+</sup> and Na<sup>+</sup> signalling in astroglia: differential filtering of extracellular cations. *Cell Calcium* 54: 120–125
- Rizzuto R, Pinton P, Carrington W, Fay FS, Fogarty KE, Lifshitz LM, Tuft RA, Pozzan T (1998) Close contacts with the endoplasmic reticulum as determinants of mitochondrial Ca<sup>2+</sup> responses. *Science* 280: 1763–1766
- Rizzuto R, De Stefani D, Raffaello A, Mammucari C (2012) Mitochondria as sensors and regulators of calcium signalling. *Nat Rev Mol Cell Biol* 13: 566–578
- Rodriguez AM, Carrico PM, Mazurkiewicz JE, Melendez JA (2000) Mitochondrial or cytosolic catalase reverses the MnSOD-dependent inhibition of proliferation by enhancing respiratory chain activity, net ATP production, and decreasing the steady state levels of H<sub>2</sub>O<sub>2</sub>. *Free Radic Biol Med* 29: 801–813
- Rosker C, Graziani A, Lukas M, Eder P, Zhu MX, Romanin C, Groschner K (2004) Ca<sup>2+</sup> signaling by TRPC3 involves Na<sup>+</sup> entry and local coupling to the Na<sup>+</sup>/Ca<sup>2+</sup> exchanger. *J Biol Chem* 279: 13696–13704
- Rudolf R, Mongillo M, Magalhaes PJ, Pozzan T (2004) In vivo monitoring of Ca<sup>2+</sup> uptake into mitochondria of mouse skeletal muscle during contraction. *J Cell Biol* 166: 527–536
- Singaravelu K, Nelson C, Bakowski D, de Brito OM, Ng SW, Di Capite J, Powell T, Scorrano L, Parekh AB (2011) Mitofusin 2 regulates STIM1 migration from the Ca<sup>2+</sup> store to the plasma membrane in cells with depolarized mitochondria. *J Biol Chem* 286: 12189–12201
- Szabadkai G, Duchon MR (2008) Mitochondria: the hub of cellular Ca<sup>2+</sup> signaling. *Physiology* 23: 84–94
- Vig M, Beck A, Billingsley JM, Lis A, Parvez S, Peinelt C, Koomoa DL, Soboloff J, Gill DL, Fleig A, Kinet JP, Penner R (2006) CRACM1 multimers form the ion-selective pore of the CRAC channel. *Curr Biol* 16: 2073–2079
- Wang X, Wang Y, Zhou Y, Hendron E, Mancarella S, Andrade MD, Rothberg BS, Soboloff J, Gill DL (2014) Distinct Orai-coupling domains in STIM1 and STIM2 define the Orai-activating site. *Nat Commun* 5: 3183



- Yang KT, Pan SF, Chien CL, Hsu SM, Tseng YZ, Wang SM, Wu ML (2004) Mitochondrial Na<sup>+</sup> overload is caused by oxidative stress and leads to activation of the caspase 3- dependent apoptotic machinery. *FASEB J* 18: 1442–1444
- Zal T, Gascoigne NR (2004) Photobleaching-corrected FRET efficiency imaging of live cells. *Biophys J* 86: 3923–3939
- Zhang SL, Yu Y, Roos J, Kozak JA, Deerinck TJ, Ellisman MH, Stauderman KA, Cahalan MD (2005) STIM1 is a Ca<sup>2+</sup> sensor that activates CRAC channels and migrates from the Ca<sup>2+</sup> store to the plasma membrane. *Nature* 437: 902–905
- Zhang SL, Yeromin AV, Zhang XH, Yu Y, Safrina O, Penna A, Roos J, Stauderman KA, Cahalan MD (2006) Genome-wide RNAi screen of Ca<sup>2+</sup> influx identifies genes that regulate Ca<sup>2+</sup> release-activated Ca<sup>2+</sup> channel activity. *Proc Natl Acad Sci USA* 103: 9357–9362
- Zhang X, Gonzalez-Cobos JC, Schindl R, Muik M, Ruhle B, Motiani RK, Bisailon JM, Zhang W, Fahrner M, Barroso M, Matrougui K, Romanin C, Trebak M (2013) Mechanisms of STIM1 activation of store-independent leukotriene C4-regulated Ca<sup>2+</sup> channels. *Mol Cell Biol* 33: 3715–3723
- Zhang H, Clemens RA, Liu F, Hu Y, Baba Y, Theodore P, Kurosaki T, Lowell CA (2014) STIM1 calcium sensor is required for activation of the phagocyte oxidase during inflammation and host defense. *Blood* 123: 2238–2249
- Zhou Y, Wang X, Wang X, Loktionova NA, Cai X, Nwokonko RM, Vrana E, Wang Y, Rothberg BS, Gill DL (2015) STIM1 dimers undergo unimolecular coupling to activate Orai1 channels. *Nat Commun* 6: 8395